in vivo, we analyzed p73 activation with brain samples of human HD patients. Western blotting with human brain samples suggested higher levels of p73 phosphorylation in HD brains than in control brains (Fig. 7 E).

Correspondingly, immunohistochemical analysis revealed an increase of phosphorylated p73 in striatal neurons of mutant Htt transgenic mice (R6/2) at 4 wk (Fig. 8, middle). It is noteworthy that antiphosphorylated p73 antibody stained both the nucleus and cytoplasm of striatal neurons in R6/2 mice (Fig. 8, middle), although anti-p73 antibody detecting both nonphosphorylated and phosphorylated p73 proteins (full-length and NH_2-terminus deletion forms) dominantly stained the cytoplasm (Fig. 8, left). On the other hand, YAPΔCs were expressed in striatal neurons of both normal and R6/2 transgenic mice, whereas the signal was relatively stronger in transgenic mice (Fig. 8, right).

Furthermore, phosphorylation of p73 was detected in striatal neurons of human HD patients (Fig. 9 A), suggesting that p73 is activated in human HD pathology. In this experiment (Fig. 9 B), because we used the antibody detecting full-length p73 but not ΔNp73, the full-length form of p73 was considered to be phosphorylated (Fig. 9 B, top). YAPΔCs were shown to exist in striatal neurons of human HD patients by a specific antibody (Fig. 9 A, bottom right) and to be colocalized with activated p73 in striatal neurons (Fig. 9 B, bottom). It is important to note that phosphorylated p73 and YAPΔCs were at very low levels in control human brains (Fig. 9 A, top). Collectively, these results suggest the possibility that p73 and YAPΔCs might be involved in the HD pathology.

YAPΔC isoforms attenuate Htt-induced neurodegeneration of *Drosophila*

Finally, we examined the in vivo effect of YAPΔCs on Htt-induced neurodegeneration in *Drosophila* models (Jackson et al., 1998). We generated more than three transgenic fly lines of human YAPΔCs. In the transgenic flies, the expression of YAPΔC protein was triggered by GMR-GAL4 that directs expression in the developing and adult eyes. To analyze the effects on photoreceptor neuron degeneration and/or the characteristic eye phenotype induced by the expression of human Htt120Q, we compared eye phenotypes between the F1 sibling flies at 10 d directly under the microscopy or by toluidine blue staining of 2-μm sections of epon-embedded eye tissues. Ommatidia structure and photoreceptor neurons were severely disrupted in GMR-Htt120Q/GMR-GAL4 double-transgenic flies (BL8533; Jackson et al., 1998), whereas the expression of YAPΔC with a 61-nt insert (YAPΔC61) markedly preserved structure in triple-transgenic flies (GMR-Htt120Q/GMR-GAL4/UAS-YAPΔC61; Fig. 10 A). Expression levels of YAPΔC61 and Htt120Q were checked in the same fly in parallel (Fig. 10 B). Quantitative analysis of rhabdomere numbers per ommatidium in four independent transgenic fly lines supported the repression of neurodegeneration by YAPΔC61 (Fig. 10 C). We observed similar improvement of neurodegeneration in other YAPΔC transgenic *Drosophila* flies (not depicted). Collectively, these in vivo data further suggest the possibility that YAPΔC isoforms might play a protective role against the toxicity of mutant Htt in HD pathology.

Discussion

In this study, we report atypical neuronal death induced by transcriptional repression (TRIAD). Transcriptional repression by Pol II–specific inhibitors leads to a very slow atypical neuronal death whose progression is clearly different from the well-known cell death prototypes. A morphological feature of TRIAD might be the vacuolization of ER, although it should be stressed that the majority of neurons (>90%) do not show remarkable morphological changes. These findings might be relevant to the roles of transcriptional disturbance in HD disease (for review see Gusella and MacDonald, 2000; Zoghbi and Orr, 2000; Ross, 2002; Taylor et al., 2002; Bates, 2003; Okazawa, 2003; Sugars and Rubinsztein, 2003). In addition, the lengthy progression of TRIAD might cast light on the basic question of why neurons stay alive under neurodegeneration for a long period.

To the best of our knowledge, there are a few atypical cell deaths that might be partially analogous to TRIAD. One is a lengthy cell death of *Dictyostelium discoideum* during sorocarp formation, in which dying cells show cytoplasmic vacuolization (Cornillon et al., 1994). The second, termed paraptosis, is induced by the overexpression of the intracellular domain of insulinlike growth factor I (IGF-I) receptor in 293T cells (Sperandio, et al., 2000). Paraptosis is characterized by vacuolization of the ER but no nuclear fragmentation, cellular blebbing, or apoptotic body formation (Sperandio, et al., 2000). These two atypical cell deaths might share molecular pathways (Wyllie and Goldstein, 2001). Although TRIAD shows a related morphological change, TRIAD is clearly different from paraptosis, as the latter is inhibited by both actinomycin D and cycloheximide (Sperandio, et al., 2000). Another point that distinguishes TRIAD from paraptosis is the cell death stimulus. Paraptosis was reported only in ectopic expression of truncated IGF-I receptor in

CDDP-induced apoptosis of MCF-7 cells. 25 μM CDDP was added to the medium 24 h after infection of adenovirus vectors, and cell death assay was performed with annexin-V (Tagawa et al., 2004) in six wells after another 16 h. Adenovirus expression vectors are abbreviated as follows: AxCA, empty adenovirus vector AxCAwt; YAP, AxCAYAP-FL; ins13, AxCAins13; ins25, AxCAins25; and ins61, AxCAins61. Right panel shows the expression of YAP insert forms in cortical neurons. (C) YAPΔCs suppressed TRIAD of cortical neurons. 24 h after infection of adenovirus vectors of YAP isoforms, 25 μg/ml AMA was added. Cell death was assayed with annexin-V (six wells) at 4 d. Right panel shows expression of YAPΔCs in cortical neurons. (D) YAPΔC suppression by siRNA specific to a YAPΔC common sequence (siYAPΔ) enhanced AMA-induced TRIAD of cortical neurons, supporting the idea that YAPΔCs repress TRIAD of cortical neurons. Right panel shows specific repression of YAPΔCs by siYAPΔ. sc, siRNA of a scrambled sequence. 0.5 μg/well siRNA was transfected into cortical neurons (2×10^4 cells/well of 24-well dish), and 25 μM AMA was added to the medium 12 h later. Cell death was quantified by trypan blue staining in six wells at 4 d. (right) Bottom numbers represent relative intensities of the endogenous YAPΔC bands. (A–D) Asterisks indicate significant differences from controls ($P < 0.01$, *t* test). Error bars represent SD. (E) p73 was activated in TRIAD of cortical neurons. Right panel shows fold increase of phosphorylated p73 by AMA treatment (25 μg/ml).

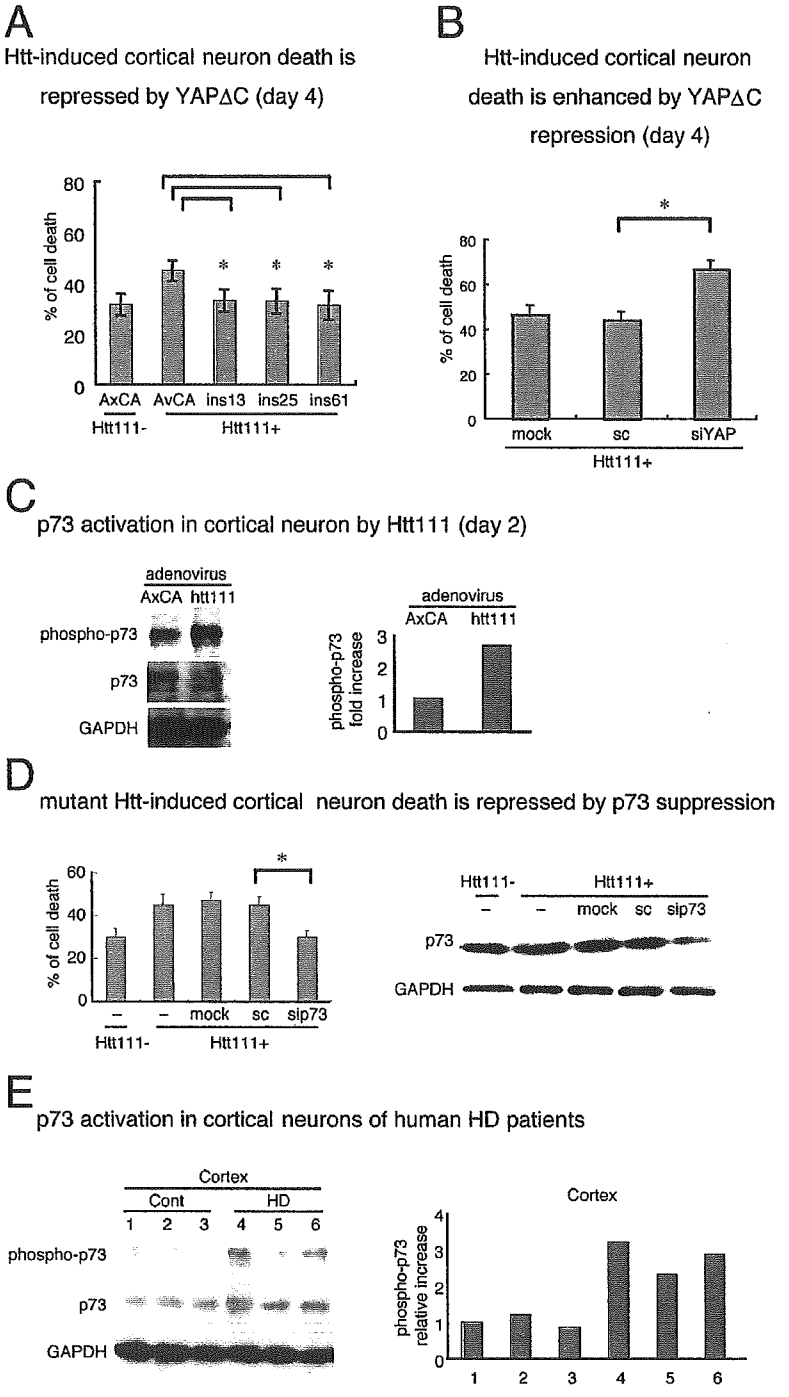

Figure 7. **Relevance of YAPΔC isoforms and p73 to Htt-induced pathology.** (A) YAPΔCs repressed Htt-induced cell death of cortical neurons. Primary cortical neurons were coinfected by adenovirus vectors for mutant Htt (AxCAHtt111) and a YAPΔC (AxCAins13, AxCAins25, or AxCAins61). Cell death was assayed with trypan blue at 4 d. As a control, empty vector (AxCA) was used. Expression of mutant Htt was equivalent among infections (not depicted). (B) Suppression of YAPΔCs by YAPΔC sequence-specific siRNA (siYAPΔ) enhanced mutant Htt-induced cell death of cortical neurons. 0.5 μg/well siRNA was transfected into primary cortical neurons (2×10^4 cells/well of 24-well dish) and infected with adenovirus vectors for mutant *htt* (AxCAHtt111) 12 h later. Cell death was quantified by trypan blue in six wells at 4 d. (C) Phosphorylation of p73 was induced in cortical neurons expressing mutant Htt. Cortical neurons were harvested 48 h after infection of empty adenovirus vector (AxCA) or mutant Htt adenovirus vector (htt111). Immunoblotting was performed with anti-p73, antiphosphorylated p73, or anti-GAPDH (glyceraldehyde-3-phosphate dehydrogenase) antibody (left). Relative values of phosphorylated p73 to total p73 were compared between AxCA-infected and AxCAHtt111-infected neurons (right). (D) Suppression of p73 by siRNA repressed Htt-induced cell death of cortical neurons (left). siRNA transfection and AxCAHtt111 infection were performed similarly to that in B. sip73, siRNA of p73; sc, siRNA of a scrambled sequence; Mock, mock treatment without siRNA. Cell death was quantified by trypan blue staining in four independent wells at 4 d after infection. Right panel shows expression of p73 and GAPDH at the time point of infection of AxCAHtt111 and indicates suppression of p73 by siRNA. (A, B, and D) Asterisks indicate significant reduction of cell death in four independent assays ($P < 0.01$, *t* test). Error bars represent SD. (E) p73 phosphorylation was enhanced in the brain of human HD patients. Cerebral cortex tissues of three HD patients (lanes 4–6) and three controls (lanes 1–3) were analyzed similarly (left). Relative values of phosphorylated p73 to total p73 were calculated (right).

nonneuronal cells (Sperandio, et al., 2000). Furthermore, the role that we find for YAP in TRIAD has not been demonstrated in paraptosis or *D. discoideum* cell death. It is noteworthy that Degterev et al. (2005) has recently reported a new type of cell death—necroptosis. They showed that in the absence of intracellular apoptotic signaling, extrinsic TNF stimulation triggers nonapoptotic cell death, showing necrotic morphology and autophagy. Although rapamycin did not increase typical LC3-negative vacuoles of TRIAD (Fig. S3) negating the autophagic component in TRIAD, we need to analyze carefully the relationship between TRIAD and necroptosis, including the viewpoint of cell death speed.

It is also necessary to consider TRIAD with previous classifications of cell death. Schweichel and Merker (1973) classified three types of cell death. Type 1 was manifested as nuclear condensation and pyknosis, reduced cytoplasmic volume, and

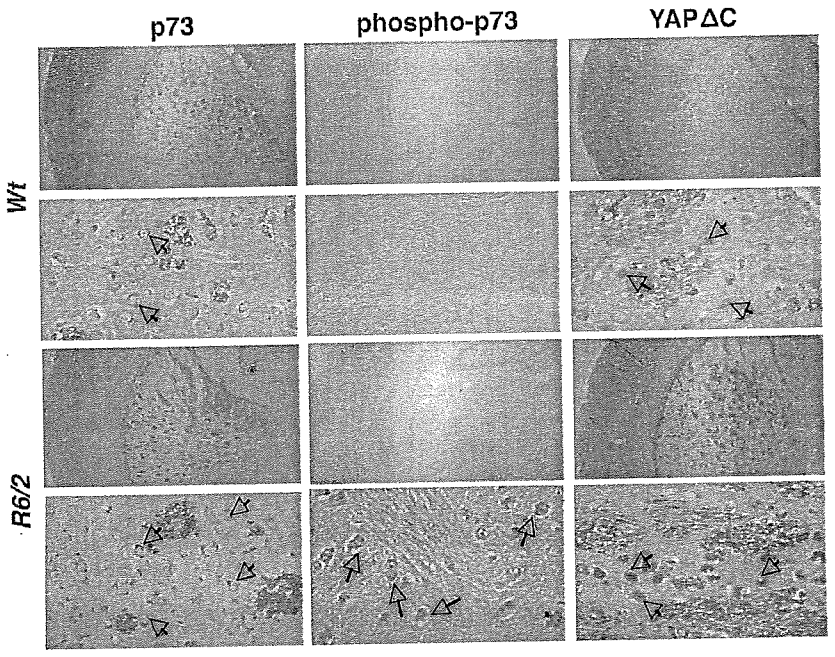

Figure 8. **YAPΔC and phosphorylated p73 are expressed in striatal neurons of Htt transgenic mice.** Immunohistochemical analyses of mutant Htt transgenic (R6/2) and sibling control mice were performed at 4 wk with anti-p73 (full-length form), antiphosphorylated p73, or anti-YAPΔC antibodies. Arrows indicate immunoreactive striatal neurons. Expression of phosphorylated p73 was increased in R6/2 transgenic mice (middle), whereas the total amount of p73 was similar in transgenic and control mice (left). Immunoreactivities of YAPΔC were slightly increased in transgenic mice (right).

late cell fragmentation/phagocytosis. Type 2 was an autophagic vacuolization in the cytoplasm, and type 3 was described as cytoplasmic cell death in which general organelle breakdown was apparent. Type 1 is apoptosis, and types 2 and 3 were necrotic (Schweichel and Merker, 1973). In 1990, Peter Clarke redefined an earlier model of cell death developed by Schweichel and Merker (Clarke, 1990). Clarke's modification was to expand the forms of cytoplasmic cell death into types 3A and 3B. 3A is a nonlysosomal breakdown, and 3B is cytoplasmic (Clarke, 1990). Cells undergoing the 3A type of cell death show an initial swelling of cytoplasmic organelles and the generation of vacuoles that eventually fuse with the extracellular space. A breakup of cell structure without autophagic or heterophagic activity occurs. In type 3B death, which is also known as the cytoplasmic form of cell death, swollen organelles (dilated perinuclear space, ER, and Golgi apparatus) are apparent as well as vacuoles. The cell membrane retracts, and the nucleus becomes karyolytic/edematous. Heterophagic elimination can occur. Type 3B has also been termed paraptosis/oncosis. Among these, TRIAD is close to type 3B. However, in addition to the aforementioned reason, TRIAD seems to be different from type 3B because vacuolization of ER is far more remarkable than morphological changes of other organelles in TRIAD.

In HD models, several studies have reported atypical cell death with cytoplasmic vacuolization. Sapp et al. (1997) reported that mutant Htt accumulates in punctate structures mimicking endosomal–lysosomal organelles of affected HD neurons. They further showed by extensive analyses, including immunoelectron microscopy, that mutant Htt appears in autophagosomes (Kegel et al., 2000). Other studies also pointed out the possible involvement of autophagy in the HD disease pathology (Nagata et al., 2004; Ravikumar et al., 2004; Iwata et al., 2005). Meanwhile, Hirabayashi et al. (2001) isolated VCP (valosin-containing protein)/p97, a member of the AAA+ family of ATPase proteins, as a HD-interacting protein. The expression of the mutant form of VCP leads to cytoplasmic vacuolization, which might be homologous to vacuoles in TRIAD because they were fused to ER (Hirabayashi et al., 2001). Collectively, although our results so far seem to negate the identity of the TRIAD vacuoles to autophagosomes, we cannot exclude the possibility that they might share certain characteristics with the vacuoles reported in HD models.

As for the molecular pathway of TRIAD, YAPΔCs and p73 might modify the process. Up- or down-regulation of YAPΔCs suppresses or enhances TRIAD in cortical neurons, respectively (Fig. 6, C and D). Together with evidence that AMA treatment increases active p73 in neurons (Fig. 6 E) and that YAPΔCs remain during TRIAD of cortical neurons (Fig. 4 G), these data suggest that p73-mediated cell death signaling might be attenuated by YAPΔCs in TRIAD. Consistently, the percentage of morphologically changed neurons (vacuole-possessing neurons) was very low. It might be a reason why TRIAD does not progress rapidly like apoptosis.

p73 was activated in human and mouse HD pathology in vivo (Figs. 8 and 9). YAPΔC isoforms were coexpressed in affected neurons of human HD patients (Fig. 9). Repression of p73 and expression of YAPΔCs attenuated Htt-induced neuronal cell death of primary neurons (Fig. 7, A and D), whereas YAPΔC repression enhanced the neuronal cell death (Fig. 7 B). Furthermore, YAPΔC isoforms suppressed neurodegeneration of photoreceptor cells of *Drosophila* in vivo (Fig. 10). These findings suggest that YAPΔCs and p73 might be relevant to the HD pathology.

p53 has been implicated in the HD pathology because p53 coaggregates with mutant Htt (Steffan et al., 2000). Bae et al. (2005) recently reported that mutant Htt interacts with,

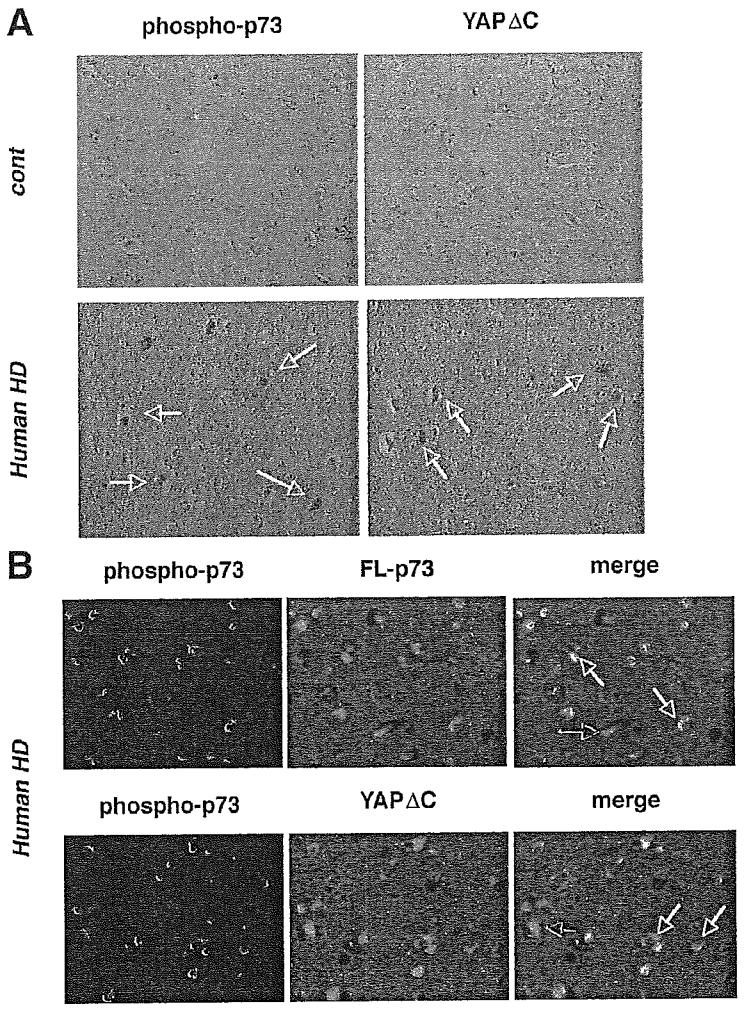

Figure 9. **YAPΔC and phosphorylated p73 are coexpressed in striatal neurons of human HD brain.** (A) Immunoreactivities of phosphorylated p73 and YAPΔC isoforms were increased in striatal neurons of HD patients (arrows). Postmortem brain tissues, including the caudate nucleus, were prepared from three HD patients and three controls. (B) Double staining with anti-p73 rabbit polyclonal antibody specific for full-length p73 but not reactive to ΔNp73 (H-79; 1:500; Santa Cruz Biotechnology, Inc.) and with antiphospho-p73 rabbit polyclonal antibody (1:500; Cell Signaling) showed colocalization of the two signals in most striatal neurons of HD patients (top, white arrows). It suggests that the full-length p73 is phosphorylated in striatal neurons. Bottom panels show that YAPΔC isoforms were colocalized with phosphorylated p73 in striatal neurons (bottom, white arrows). However, a minor portion of neurons expresses only p73 (red arrows).

translocates, and activates p53. They also showed that mating mutant Htt transgenic mice with p53-null mice ameliorates neurological symptoms by mutant Htt (Bae et al., 2005). These results suggest that p53 activation promotes the HD pathology. Because p73 and p53 belong to the same family of transcription factors recognizing a similar consensus sequence on genomic DNA (for review see Irwin and Miller, 2004), the common cascade shared by the two factors should be investigated in the HD pathology. For instance, upstream signals activating these two factors and target gene activation by these transcription factors in the HD pathology should be analyzed in the future. On the other hand, because p53 is suggested to have a direct effect on mitochondria (Mihara et al., 2003), it might be necessary to test whether p73 also plays a similar role.

It is important to note that hyperactive p73 could trigger vacuolar changes of ER in nonneuronal cells (Terrinoni et al., 2004). If this is true, the vacuole formation in TRIAD might be triggered by activated p73. In this case, although ER stress could be induced by mutant polyQ protein (Kouroku et al., 2002; Nishitoh et al., 2002), ER stress might also be evoked by a signal from the nucleus in parallel. Investigation on the possible connection between the nucleus and ER might contribute to understanding the polyQ pathology. The hypothetical pathway should be examined and elucidated in the future. In summary, our results present a novel model of cell death that might cast more light on the HD pathology.

Materials and methods

Primary neuron culture

Cerebral cortex tissues isolated from E17 Wistar rat embryos and cerebellar tissues isolated from P7 Wistar rat pups were minced (with razors) and treated with 0.25% trypsin (Invitrogen) in PBS, pH 7.5, at 37°C for 20 min with gentle shaking every 5 min. After stopping the reaction with DME containing 50% FBS, DNase I (Boehringer) was added to the solution at a final concentration of 100 μg/ml, and tissues dissociated gently by pipetting with blue tips. Cells filtered by nylon mesh (pore size of 70 mm; Falcon; BD Biosciences) were collected by centrifugation, resuspended in DME supplemented with 20 mM glucose, 16 mM sodium bicarbonate, 4 mM glutamine, 25 μg/ml gentamicin, and 10% FBS, and plated on 24-well dishes (Corning) coated by poly-L-lysine (Sigma-Aldrich) at 3×10^5 cells/well. 12 h after plating, cytosine arabinoside was added to the culture medium at 4 M of final concentration to prevent the growth of glial cells. Cerebellar neurons were cultured at high potassium (25 mM) ordinarily but were cultured at 5.4 mM potassium to induce apoptosis. Cortical neurons were cultured at low potassium condition (5.4 mM). Necrosis of cortical neurons

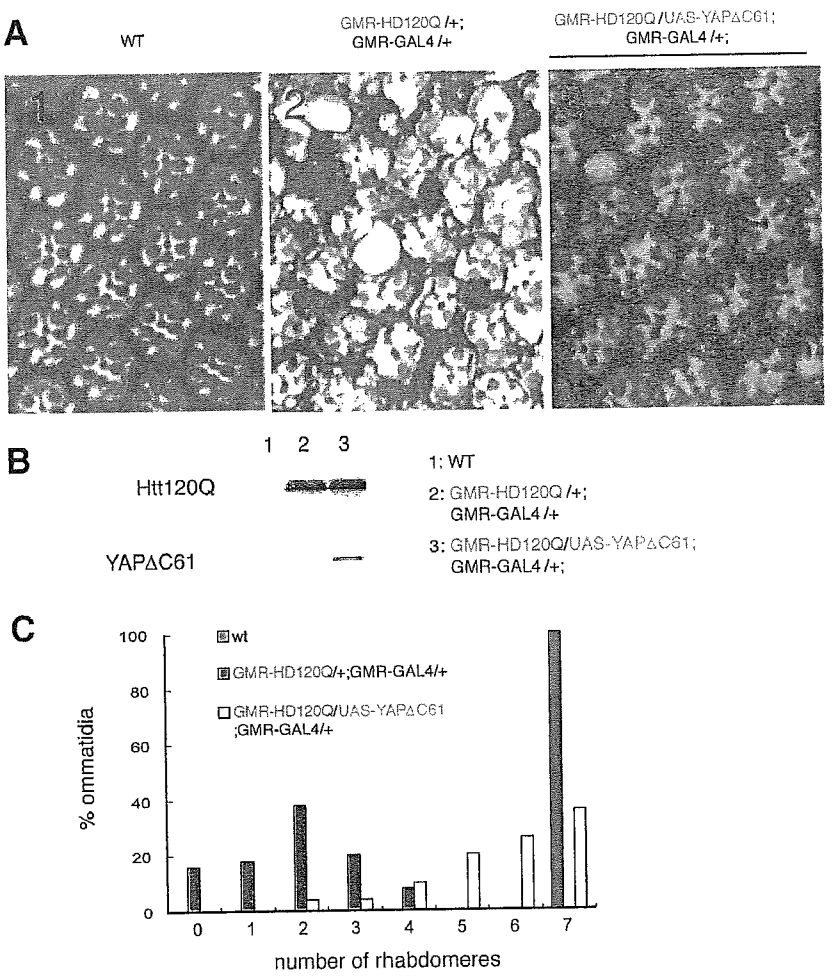

Figure 10. **YAPΔC represses neurodegeneration of *Drosophila* ommatidia.** (A) Morphological analyses of photoreceptor cells in cross sections of *Drosophila* ommatidia. In wild type (WT), a single ommatidium possesses seven rhabdomeres aligned regularly, whereas ommatidia structure and photoreceptor neurons were severely destructed in Htt120Q transgenic flies (GMR-HD120Q/+;GMR-GAL4/+). Expression of YAPins61 remarkably improved the structural anomalies (GMR-HD120Q/UAS-YAΔ61;GMR-GAL4/+). (B) Expression levels of Htt120Q and YAPΔC61 were examined by Western blot analysis in the same fly as shown in Fig. 7 A. (C) Quantitative analysis of rhabdomere numbers per ommatidium in WT, Htt120Q transgenic flies (GMR-HD120Q/+; GMR-GAL4/+), and a representative line of transgenic flies (GMR-HD120Q/UAS-YAPΔ61;GMR-GAL4/+) supported the repression of neurodegeneration by YAPΔC61. More than 30 ommatidia were analyzed in three flies from a line. The results with other three lines of transgenic flies (GMR-HD120Q/UAS-YAPΔ61;GMR-GAL4/+) were basically similar (not depicted).

was induced by the freeze and thaw treatment. To induce TRIAD, AMA (Sigma-Aldrich) was added to the medium at a final concentration of 10 or 25 μg/ml, except for dose–response survival experiments in which the final concentration was 10–250 μg/ml. Actinomycin D (Sigma-Aldrich) was added to the medium at 0.1, 0.5, or 2.5 μg/ml.

Cell death assay

Cell death assays were performed either by trypan blue dye exclusion assay or MTT assay as described in each figure legend. For trypan blue assay, cells were incubated for 5 min in 0.4% trypan blue (Invitrogen). Blue-stained (nonviable) and nonstained (viable) cells were counted (at least 2,000 cells for each condition) in 10–20 visual fields randomly selected at 100× from each of three dishes, as described previously (Tagawa et al., 2004). MTT assay was performed with MTT cell proliferation/viability assay (R&D Systems) according to the commercial protocol. At each time point, the value of drug-treated cells was corrected to the value of nontreated cells as 100%.

Acquisition and processing of microscopic images

Regarding electron microscopic observation, cells were washed with PBS three times, fixed in 2.5% glutaraldehyde/0.1 M phosphate buffer, and treated with 1% OsO_4/0.1 M phosphate buffer for 2 h. Fixed cells were dehydrated through a graded ethanol series and embedded in epoxy resin. Ultrathin sections were stained with uranyl acetate and lead citrate and examined with a transmission electron microscope (H-9000; Hitachi) at 24°C (5,000–50,000×). Numerical aperture of the objective lens was 4, and the imaging medium was air. Data acquisition was performed by electron microscope film.

As for immunocytochemistry, stained cells were observed with a microscope (IX-71; Olympus) at RT (20 or 40×; NA 0.40 or 0.60, respectively), and the imaging medium was air. Data acquisition was performed with a camera (C4742-95-12ERG; Hamamatsu), a controller (ORCA-ER; Hamamatsu), and AQUACOSMOS software (Hamamatsu). The fluorochromes will be described in each method.

Analysis of autophagy

24 h after transfection of pEGFP-LC3, HeLa cells were treated with 10 μg/ml AMA and observed by fluorescence microscopy (Fig. 2). To further analyze the relationship between LC3-positive phagosomes and AMA-induced vacuoles, autophagy was induced by 200 ng/μl rapamycin for 2 h (Sigma-Aldrich; for review see Klionsky and Emr, 2000). LC3-positive and -negative vacuoles were counted in the presence or absence of AMA. HeLa cells were transfected with pEGFP-LC3 by SuperFect (QIAGEN), collected 36 h after transfection, and subjected to Western blot analysis. Anti-EGFP polyclonal antibody (BD Living Colors) and anti-LC3 antibody were used at dilutions of 1:1,000 and 1:2,000, respectively. pEGFP-LC3 and anti-LC3 antibody were gifts from T. Yoshimori (National Institute of Genetics, Mishima, Japan) and N. Mizushima (Tokyo Metropolitan Institute for Medical Science, Tokyo, Japan).

Identification of AMA-induced vacuolization

After treatment of AMA (Sigma-Aldrich) for 6 h, HeLa cells were washed with PBS and fixed using 4% PFA for 15 min at RT. Cells were incubated for 1 h at RT with the following primary antibodies: anti-CCO1 mouse monoclonal antibody (1:100; Invitrogen); anti-EEA1 mouse monoclonal antibody (1:100; Transduction Laboratories); anti-Golgi58k mouse monoclonal antibody (1:100; Sigma-Aldrich); and anti-CD63 (1:100; Cymbus Biotechnology Ltd.). Secondary antibodies conjugated with AlexaFluor488 (Invitrogen) were used at a dilution of 1:1,000 and hybridized for 30 min at RT. HeLa cells were transfected by pEGFP-LC3 (a gift of N. Mizushima and

T. Yoshimori; Kabeya et al., 2000) or pECFP-ER (BD Biosciences) using Superfect (QIAGEN) according to the manufacturer's instructions.

Western blot analyses of caspase-3, -7, and -12

Primary neurons were treated with 25 μg/ml AMA as indicated and were dissolved in 62.5 mM Tris-HCl, pH 6.8, 2% (wt/vol) SDS, 2.5% (vol/vol) 2-mercaptoethanol, 5% (vol/vol) glycerin, and 0.0025% (wt/vol) bromophenol blue on culture dishes. Positive controls for caspase-3 and -7 were prepared from HeLa cells treated with 1 μM staurosporin (Sigma-Aldrich) for 5 h. For a caspase-12 control, HeLa cells were treated with 20 μM A23187 (Calbiochem) for 24 h. Primary and secondary antibodies were diluted as follows: anticaspase-3 polyclonal rabbit antibody (Cell Signaling) at 1:1,000; anticaspase-6 polyclonal antibody (Cell Signaling) at 1:500; anticaspase-7 polyclonal antibody (Cell Signaling) at 1:500; anticaspase-12 polyclonal antibody (14F7; Sigma-Aldrich) at 1:1,000; HRP-conjugated anti–rabbit IgG (GE Healthcare) at 1:3,000; and HRP-conjugated anti–rat IgG (Sigma-Aldrich) at 1:20,000.

Cytochrome c release

10^7 primary cortical neurons were treated with 10 μg/ml AMA as indicated (Fig. 3 C). As a positive control, the same amount of primary cortical neurons were treated with 1 μM staurosporin (Sigma-Aldrich) for 8 h. The cells were washed twice with ice-cold PBS on the dish, collected, and suspended in 500 μl of ice-cold buffer (20 mM Hepes, pH 7.4, 10 mM KCl, 1.5 mM $MgCl_2$, 1 mM EDTA, 1 mM DTT, 1 mM PMSF, and 250 mM sucrose) and disrupted by moderate strokes in a homogenizer. The homogenate was centrifuged twice at 1,300 *g* for 5 min to remove nuclei, unbroken cells, and large membrane fragments. From the supernatant, mitochondria were isolated by further centrifugation at 17,000 *g* and 4°C for 15 min. Pellets were dissolved in the sample buffer described above, separated by 15% SDS-PAGE, blotted to polyvinylidene difluoride membranes (Fine Trap; Nihon Eido), incubated with cytochrome c monoclonal antibody (1:1,000; Santa Cruz Biotechnology, Inc.), and subjected to HRP-coupled detection. The supernatant of the final centrifugation was used as a cytosolic fraction.

RNA probes for microarray analyses

Cells in culture dishes are harvested in TRIzol reagent (Invitrogen) after rinsing with PBS twice, and total RNA was prepared according to the manufacturer's protocol. Labeling and amplification of RNA was performed using the Agilent Fluorescent Linear Amplification Kit (G2554A; Agilent Technologies) according to the manufacturer's protocol. First, double-stranded cDNAs with a T7 promoter were synthesized from 2 μg of total RNA by Moloney murine leukemia virus reverse transcriptase using an oligonucleotide dT-primer, which contains the T7 promoter sequence, and random hexamers (40°C for 4 h). Then, using these double-stranded cDNAs as templates, cRNA was synthesized by T7 RNA polymerase using Cy3- or Cy5-labeled CTP (40°C for 1 h). cRNAs from AMA-treated cortical neurons, AMA-treated cerebellar neurons, or low potassium–exposed cerebellar neurons were labeled with Cy3 or Cy5. Synthesized cRNA was precipitated with lithium chloride, ethanol rinsed, and dissolved in nuclease-free water. To check the quality of cRNA, OD_{260}, OD_{280}, A_{552} (for Cy3), and A_{650} (for Cy5) measurements were taken. Then, OD_{260}/OD_{280}, amplification rates and dye incorporation rates (pmol/μg RNA) of cRNA were calculated. Using these criteria, we found that our samples were of high quality (OD_{260}/OD_{280}, <2.0; amplification rate, <400; Cy3 incorporation, <15 [pmol/μg RNA]; and Cy5 incorporation, <12 [pmol/μg RNA]).

Microarray analysis

Hybridization procedures were performed using the In situ Hybridization Kit Plus (5184–3568; Agilent Technologies) according to the manufacturer's protocol. First, Cy3- and Cy5-labeled cRNAs (1 μg each) were mixed and incubated with fragmentation buffer (Agilent Technologies) at 60°C for 30 min. Mouse Development Oligo Microarray (G4120A; Agilent Technologies), which contains 20,371 60-mer oligonucleotides from mouse cDNA, was hybridized with fragmented cRNA targets at 60°C for 17 h using CHBIO (Hitachi). Hybridized microarrays were rinsed twice and dried by spraying N_2 gas (99.999%) using a filter-equipped air gun (mycrolis KK; Nihon).

Fluorescent signals were read using a microarray scanner (CRBIO IIe; Hitachi). Data were analyzed using analysis software (DNASIS array; Hitachi). In brief, data either from control spots or from spots containing high intensities of artificial signals were removed. Then, the signal intensity of each spot was normalized to equalize total signal intensity. Normalized signal intensity of each spot was plotted on a scatter plot with Cy3 fluorescence on the y axis and Cy5 fluorescence on the x axis. The ratio of Cy3/Cy5 fluorescence was calculated, and genes with outstanding Cy3/Cy5 ratios of >2.0 or <0.5 were listed.

To confirm the results, we also used a rat cDNA microarray (G4105A; Agilent Technologies) on which cDNAs (mean length of 500 bases) derived from 14,811 genes were spotted. cDNA probes were labeled by the Direct Label Kit (G2557A; Agilent Technologies) with an oligonucleotide dT primer according to the manufacturer's protocol. The chips were hybridized at 65°C for 17 h and washed with 0.5× SSC and 0.01% SDS for 5 min at RT and with 0.06× SSC for 2 min at RT.

PCR cloning

RT-PCR cloning of YAP was conducted with cDNA reverse transcribed from 1 mg of total RNA prepared from rat cortical neurons by using the RNA LA PCR Kit (Takara) and primers F (5′-GGAATTCTATGGAGCCCGCGCAA-3′) and R (5′-ACGCGTCGACCTATAACCACGTGAG-3′). PCR amplification was performed for 35 cycles (94°C for 30 s, 52°C for 30 s, and 72°C for 90 s). The resultant cDNAs were subcloned between EcoRI and SalI sites of pBluescriptII SK+. Nucleotide sequences were determined by using M13 or synthesized internal primers and the ABI PRISM BigDye Terminator Cycle Sequencing Kit version 3.1 (Applied Biosystems) and ABI PRISM 310 DNA Sequencer (Applied Biosystems). pBluescript plasmids containing 13-, 25- and 61-nt insert forms of YAP were named pBSins13, pBSins25, and pBSins61, respectively. The cDNA of each YAP insert was subcloned into pCI neo (Promega) and denoted pClins13, pClins25, and pClins61, respectively.

Luciferase assay

5×10^6 cells MCF-7 cells were transiently transfected with 5 μg of pGL3-Bax-Luc (Strano et al., 2002) with pCI–FL-YAP, -YAPΔC (pClins13, pClins25, and pClins61), or control pCI-neo using LipofectAMINE 2000 (Invitrogen) according to the protocol described previously (Basu et al., 2003).

Western blot analysis

Cells were resuspended in 62.5 mM Tris-HCl, pH 6.8, 2% (wt/vol) SDS, 2.5% (vol/vol) 2-mercaptoethanol, 5% (vol/vol) glycerin, and 0.0025% (wt/vol) bromophenol blue on culture dishes. Cell lysates prepared from wells containing either 3.3×10^4 HeLa cells or 1.0×10^5 primary neurons were subject to SDS-PAGE gels, transferred onto polyvinylidene difluoride membranes (Fine Trap; Nihon Eido), incubated with each primary antibody for 1 h and the corresponding HRP-conjugated secondary antibody for 30 min, and visualized using the ECL Western Blotting Detection System (GE Healthcare). The dilution conditions for primary and secondary antibodies were as follows: anti-YAP polyclonal rabbit antibody (H-125; Santa Cruz Biotechnology, Inc.) at 1:1,000; anti-GAPDH mouse monoclonal antibody (Chemicon) at 1:100,000; HRP-conjugated anti–mouse IgG (GE Healthcare) at 1:5,000; and HRP-conjugated anti–rabbit IgG (GE Healthcare) at 1:3,000. Anti-YAPΔC rabbit polyclonal antibody was raised against the common COOH-terminal peptide (SVFSRDDSGIEDNDNQ) by immunizing rabbits and was used for Western blotting at a 1:1,000 dilution.

Adenovirus vector construction

The replication-defective adenovirus vectors were constructed by using the Adenovirus Expression Vector Kit (Takara) according to the manufacturer's instructions. In brief, cDNAs of YAP isoforms were digested with EcoRI and SalI from pBSYAP-FL (containing rat FL-YAP), pBSins13, pBSins25, and pBSins61. Ends were blunted using the blunting high kit (Toyobo), and each insert was subcloned into the SwaI site of the pAxCAwt cosmid (Takara). The resultant cosmids were transfected into 293T cells by the calcium-phosphate method with digested DNA of adenovirus and the medium containing dead cells recovered as the virus solution. After two or three rounds of amplification (5×10^8 and $\sim 5 \times 10^9$ plaque-forming units/ml), clonality was checked by restriction with endonucleases and PCR. We designated the adenovirus vectors AxCAYAP-FL, AxCAins13, AxCAins25, and AxCAins61. The vectors were used for infection of HeLa cells and primary neurons at a multiplicity of infection (MOI) of 100. Preliminary examination of the efficiency of protein expression and toxicity of adenovirus was performed by infecting primary neurons with a vector for EGFP and a mock vector at multiple MOI, respectively. More than 90% of the neurons expressed EGFP at an MOI of 100. The difference in cell death percentage between noninfected and mock-infected neurons estimated by trypan blue staining was <3% when the MOI did not exceed 500.

Northern blotting

10 μg of total RNA from primary culture neurons was subjected to electrophoresis using a MOPS/formaldehyde gel. Separated RNAs were

capillary blotted to Hybond-N (GE Healthcare) and fixed by UV cross-linking (120,000 μJ/cm^2). Full-length cDNA of ins61 was digested from pB-Sins61, purified from gel, and radiolabeled using α-[^{32}P]dCTP (GE Healthcare) and a random primer DNA labeling kit (Takara). ^{32}P-labeled probes were hybridized to nylon membrane at 60°C overnight with shaking. Hybridized membrane was rinsed with 1× SSC, 0.1% SDS at 50°C for 20 min twice, and with 0.1× SSC and 0.1% SDS at 60°C for 20 min twice. The membrane was then exposed to X-ray film for an appropriate time at −80°C.

RNA interference

Cells were transfected with siRNA oligonucleotides by RNAiFect (QIAGEN) according to the manufacturer's instructions. 2.5 × 10^4 cells in six-well dishes were infected at 0.5 μg siRNA/well 24 h after plating. 24 h after infection, AMA was added to a final concentration of 10 μg/m. The cell death assay was performed after another 24 h. Sequences of siRNAs of YAP and p73 were the same as those published previously (Basu et al., 2003). Sequences of the YAPΔC isoform-specific siRNAs were 5′-r(ACCG-TCAGAGCGGGAATTAGCTC)d(TT)-3′ and 5′-r(GAGCTAATTCCCGCTCT-GACGGT)d(TT)-3′, corresponding to the common exon among three YAPΔC isoforms.

Analysis of p73 phosphorylation

HeLa cells and cortical neurons were treated with 10 μg/ml AMA for 6 h and 2 d, respectively. For the Htt experiments, HeLa cells and primary cortical neurons were harvested 2 d after infection. HeLa cells or primary cortical neurons were dissolved in TNE buffer (10 mM Tris-HCl, pH 7.8, 1% NP-40, 0.15 M NaCl, 1 mM EDTA, 10 μg/ml aprotinin, 1 mM PMSF, 1 mM Na_3VO_4, and 1 mM NaF), and the supernatant was collected after centrifugation. Nonspecific binding proteins were removed by preincubation with protein G–Sepharose beads (GE Healthcare), and anti-p73 goat polyclonal antibody (S-20; Santa Cruz Biotechnology, Inc.) was added to the supernatant at 1:200. The mixture was incubated overnight at 4°C and precipitated by protein G–Sepharose beads for 1 h at 4°C. After washing five times with TNE, the precipitate was boiled in 2× loading buffer and subjected to Western blot analysis. The filter was blotted with the anti-p73 goat polyclonal antibody (S-20; 1:1,000; Santa Cruz Biotechnology, Inc.) or antiphosphorylated p73 rabbit polyclonal antibodies (1:1,000; Cell Signaling) followed by HRP-coupled detection. For analysis of p73 phosphorylation in human brain, each sample of striatum was homogenized in 20× vol TNE and subjected to the detection of p73 phosphorylation by Western blotting and immunohistochemistry.

Immunohistochemistry of transgenic mouse brains

Brain tissues were prepared from 4-wk-old R6/2 transgenic mice and the littermates. After deparaffinization and rehydration, the sections were incubated sequentially with 3% hydrogen peroxide for 30 min to inhibit endogenous peroxidase, 1.5% normal goat serum in PBS for 1 h at RT, and either a rabbit polyclonal antibody specific for full-length p73 that was raised against the NH_2-terminal 80 amino acids of p73 (H-79; 1:100; Santa Cruz Biotechnology, Inc.), an antiphospho-p73 rabbit polyclonal antibody (1:50; Cell Signaling), or an anti-YAPΔC rabbit polyclonal antibody against the common COOH-terminal peptide (SVFSRDDSGIEDNDNQ) of YAPΔC isoforms (1:100). These incubations were overnight at 4°C. The slides were incubated with anti–rabbit EnVision conjugates of secondary antibody (DakoCytomation) for 1 h at RT and visualized with DAB (Sigma-Aldrich). The same protocol was applied for immunohistochemistry of human brain sections. For double staining, each section after the first staining was agitated in stripping buffer (0.05 M glycine-HCl, pH 3.6) for 3 h at RT, hybridized with anti–glial fibrillary acidic protein polyclonal antibody (1:1,000; Chemicon) overnight at 4°C and with anti–rabbit EnVision conjugates of secondary antibody (DakoCytomation) for 1 h at RT, and visualized with DAB (Sigma-Aldrich) containing $NiCl_2$ $6H_2O$.

Immunohistochemistry of human brain samples

Postmortem brain tissues were prepared from HD patients diagnosed by CAG repeat expansion. The paraffin-embedded section was deparaffinized, rehydrated, and blocked with 5% skim milk in PBS for 30 min at RT. Single staining was performed as described in the previous section. For double staining, the section was incubated with anti-p73 rabbit polyclonal antibody specific for full-length p73 (H-79; 1:500; Santa Cruz Biotechnology, Inc.) or with or an anti-YAPΔC rabbit polyclonal antibody overnight at 4°C, washed with TNT (0.1% Tween 20–TBS) buffer twice, incubated with HRP-conjugated secondary antibody (1:3,000; GE Healthcare) for 1 h at RT, washed with TNT buffer twice, and visualized by incubation with FITC-tyramide (1:200; PerkinElmer) for 10 min. The tyramide complex was stripped off by incubation with 0.05 M glycine-HCl, pH 3.6, for 3 h at RT. After complete stripping, antiphospho-p73 rabbit polyclonal antibody (1:500; Cell Signaling) was hybridized and visualized with Cy3-conjugated secondary antibody (1:1,000; Chemicon).

***Drosophila* genetics**

Fly culture and mating were carried at 25 and 60% humidity. P{GMR-GAL4} (BL8121) and P{GMR-HD120Q} (BL8533) (Jackson et al., 1998) were obtained from the Bloomington Stock Center. The UAS-YAPins13, 25, and 61 transgenic flies were generated by cloning the corresponding human cDNA into pUAST transformation vector and injecting the construct DNA into cantonized w(cs10) (Dura et al., 1993) by standard methods (Rubin and Spradling, 1982). Genotypes of the YAP transgenic flies were determined by mating them with double balancer flies, and they were kept with a balancer gene before use. To analyze the effects of YAPins61 on photoreceptor neuron degeneration and/or the characteristic eye phenotype induced by the expression of human Htt 120Q, we compared eye phenotypes between the F1 sibling flies (GMR-HD120Q/UAS-YAPΔ61;GMR-GAL4/+ vs. GMR-HD120Q/+; GMR-GAL4/+) directly under the microscopy VH5000 (Keyence) or by toluidine blue staining of 2-μm sections of epon-embedded eye tissues.

***Drosophila* histology**

For sections of fly photoreceptor neurons, adult heads (0–10 d) were prefixed overnight in 2% formaldehyde and 2.5% glutaraldehyde in 0.1 M phosphate buffer overnight at 4%, postfixed in 1% osmium at RT for 3 h followed by dehydration in ethanol and embedding in epon for vertical and transversal semi-thin sections (2 μm), and stained with toluidine blue. At least five individuals were examined in each fly line and at each time point.

Online supplemental materials

Fig. S1 shows an MTT assay of TRIAD. Fig. S2 shows immunocytochemical analysis of TRIAD-associated vacuoles. Fig. S3 shows that TRIAD is neither autophagy nor apoptosis. Fig. S4 shows that actinomycin D also induced TRIAD. Fig. S5 shows transcriptome analysis of TRIAD. Online supplemental material is available at http://www.jcb.org/cgi/content/full/jcb.200509132/DC1.

We thank Dr. Andrew H. Wyllie for critical comments and Dr. Kathleen Isacson for naming of the new neuronal death. We thank Dr. Masao Shibata and Ms. Hiroko Ueda for their support in antibody generation and electron microscope analysis, respectively.

This work was supported by grants from the Japan Ministry of Education, Culture, Science, Sports and Technology (16650076); Japan Society for the Promotion of Science (16390249); Japan Science and Technology Agency (Precursory Research for Embryonic Science and Technology); the National Institutes of Health; and the Human Frontier Science Program.

Submitted: 21 September 2005
Accepted: 9 January 2006

References

Bae, B.-I.I., H. Xu, S. Igarashi, M. Fujimoto, N. Agrawal, Y. Taya, S.D. Hayward, T.H. Morgan, C. Montell, C.A. Ross, et al. 2005. p53 mediates cellular dysfunction and behavioral abnormalities in Huntington's disease. *Neuron.* 47:29–41.

Basu, S., N.F. Totty, M.S. Irwin, M. Sudol, and J. Downward. 2003. Akt phosphorylates the Yes-associated protein, YAP, to induce interaction with 14-3-3 and attenuation of p73-mediated apoptosis. *Mol. Cell.* 11:11–23.

Bates, G. 2003. Huntingtin aggregation and toxicity in Huntington's disease. *Lancet.* 361:1642–1644.

Bushnell, D.A., P. Cramer, and R.D. Kornberg. 2002. Structural basis of transcription: alpha-amanitin-RNA polymerase II cocrystal at 2.8 A resolution. *Proc. Natl. Acad. Sci. USA.* 99:1218–1222.

Clarke, P.G. 1990. Developmental cell death: morphological diversity and multiple mechanisms. *Anat. Embryol. (Berl.).* 181:195–213.

Cramer, P., D.A. Bushnell, and R.D. Kornberg. 2001. Structural basis of transcription: RNA polymerase II at 2.8 angstrom resolution. *Science.* 292:1863–1876.

Cornillon, S., C. Foa, J. Davoust, N. Buonavista, J.D. Gross, and P. Goldstein. 1994. Programmed cell death in *Dictyostelium*. *J. Cell Sci.* 107:2691–2704.

Degterev, A., Z. Huang, M. Boyce, Y. Li, P. Jagtap, N. Mizushima, G.D. Cuny, T.J. Mitchison, M.A. Moskowitz, and J. Yuan. 2005. Chemical inhibitor

of nonapoptotic cell death with therapeutic potential for ischemic brain injury. *Nat. Chem. Biol.* 1:112–119.

Dura, J.M., T. Preat, and T. Tully. 1993. Identification of linotte, a new gene affecting learning and memory in *Drosophila melanogaster*. *J. Neurogenet.* 9:1–14.

Gusella, J.F., and M.E. MacDonald. 2000. Molecular genetics: unmasking polyglutamine triggers in neurodegenerative disease. *Nat. Rev. Neurosci.* 1:109–115.

Hirabayashi, M., K. Inoue, K. Tanaka, K. Nakadate, Y. Ohsawa, Y. Kamei, A.H. Popiel, A. Sinohara, A. Iwamatsu, Y. Kimura, et al. 2001. VCP/p97 in abnormal protein aggregates, cytoplasmic vacuoles, and cell death, phenotypes relevant to neurodegeneration. *Cell Death Differ.* 8:977–984.

Hoshino, M., K. Tagawa, T. Okuda, and H. Okazawa. 2004. General transcriptional repression by polyglutamine disease proteins is not directly linked to the presence of inclusion bodies. *Biochem. Biophys. Res. Commun.* 313:110–116.

Irwin, M.S., and F.D. Miller. 2004. p73: regulator in cancer and neural development. *Cell Death Differ.* 11:S17–S22.

Iwata, A., J.C. Christianson, M. Bucci, L.M. Ellerby, N. Nukina, L.S. Forno, and R.R. Kopito. 2005. Increased susceptibility of cytoplasmic over nuclear polyglutamine aggregates to autophagic degradation. *Proc. Natl. Acad. Sci. USA.* 102:13135–13140.

Jackson, G.R., I. Salecker, X. Dong, X. Yao, N. Arnheim, P.W. Faber, M.E. MacDonald, and S.L. Zipursky. 1998. Polyglutamine-expanded human huntingtin transgenes induce degeneration of *Drosophila* photoreceptor neurons. *Neuron.* 21:633–642.

Jones, G.H. 1976. RNA synthesis in *Streptomyces* antibiotics: in vitro effects of actinomycin and transcriptional inhibitors from 48-h cells. *Biochemistry.* 15:3331–3341.

Kabeya, Y., N. Mizushima, T. Ueno, A. Yamamoto, T. Kirisako, T. Noda, E. Kominami, Y. Ohsumi, and T. Yoshimori. 2000. LC3, a mammalian homologue of yeast Apg8p, is localized in autophagosome membranes after processing. *EMBO J.* 19:5720–5728.

Katsuno, M., H. Adachi, M. Doyu, M. Minamiyama, C. Sang, Y. Kobayashi, A. Inukai, and G. Sobue. 2003. Leuprorelin rescues polyglutamine-dependent phenotypes in a transgenic mouse model of spinal and bulbar muscular atrophy. *Nat. Med.* 9:768–773.

Kegel, K.B., M. Kim, E. Sapp, C. McIntyre, J.G. Castano, N. Aronin, and M. Difiglia. 2000. Huntingtin expression stimulates endosomal-lysosomal activity, endosome tubulation, and autophagy. *J. Neurosci.* 20:7268–7278.

Kimura, H., K. Sugaya, and P.R. Cook. 2002. The transcription cycle of RNA polymerase II in living cells. *J. Cell Biol.* 159:777–782.

Klement, I.A., P.J. Skinner, M.D. Kaytor, H. Yi, S.M. Hersch, H.B. Clark, H.Y. Zoghbi, and H.T. Orr. 1998. Ataxin-1 nuclear localization and aggregation: role in polyglutamine-induced disease in SCA1 transgenic mice. *Cell.* 95:41–53.

Klionsky, D.J., and S.D. Emr. 2000. Autophagy as a regulated pathway of cellular degradation. *Science.* 290:1717–1721.

Kouroku, Y., E. Fujita, A. Jimbo, T. Kikuchi, T. Yamagata, M.Y. Momoi, E. Kominami, K. Kuida, K. Sakamaki, S. Yonehara, et al. 2002. Polyglutamine aggregates stimulate ER stress signals and caspase-12 activation. *Hum. Mol. Genet.* 11:1505–1515.

Melino, G., F. Bernassola, M. Ranalli, K. Yee, W.X. Zong, M. Corazzari, R.A. Knight, D.R. Green, C. Thompson, and K.H. Vousden. 2004. p73 Induces apoptosis via PUMA transactivation and Bax mitochondrial translocation. *J. Biol. Chem.* 279:8076–8083.

Mihara, M., S. Erster, A. Zaika, O. Petrenko, T. Chittenden, P. Pancoska, and U.M. Moll. 2003. p53 has a direct apoptogenic roleat the mitochondria. *Mol. Cell.* 11:577–590.

Nagata, E., A. Sawa, C.A. Ross, and S.H. Snyder. 2004. Autophagosome-like vacuole formation in Huntington's disease lymphoblasts. *Neuroreport.* 15:1325–1328.

Ni, Z., B.E. Schwartz, J. Werner, J.R. Suarez, and J.T. Lis. 2004. Coordination of transcription, RNA processing, and surveillance by P-TEFb kinase on heat shock genes. *Mol. Cell.* 13:55–65.

Nishitoh, H., A. Matsuzawa, K. Tobiume, K. Saegusa, K. Takeda, K. Inoue, S. Hori, A. Kakizuka, and H. Ichijo. 2002. ASK1 is essential for endoplasmic reticulum stress-induced neuronal cell death triggered by expanded polyglutamine repeats. *Genes Dev.* 16:1345–1355.

Okazawa, H. 2003. Polyglutamine diseases: a transcription disorder? *Cell. Mol. Life Sci.* 60:1427–1439.

Okazawa, H., J. Shimizu, M. Kamei, I. Imafuku, H. Hamada, and I. Kanazawa. 1996. Bcl-2 inhibits retinoic acid-induced apoptosis during the neural differentiation of embryonal stem cells. *J. Cell Biol.* 132:955–968.

Okazawa, H., T. Rich, A. Chang, X. Lin, M. Waragai, M. Kajikawa, Y. Enokido, A. Komuro, S. Kato, M. Shibata, et al. 2002. Interaction between mutant ataxin-1 and PQBP-1 affects transcription and cell death. *Neuron.* 34:701–713.

Ravikumar, B., C. Vacher, Z. Berger, J.E. Davies, S. Luo, L.G. Oroz, F. Scaravilli, D.F. Easton, R. Duden, C.J. O'Kane, and D.C. Rubinsztein. 2004. Inhibition of mTOR induces autophagy and reduces toxicity of polyglutamine expansions in fly and mouse models of Huntington's disease. *Nat. Genet.* 36:585–595.

Ross, C.A. 2002. Polyglutamine pathogenesis: emergence of unifying mechanisms for Huntington's disease and related disorders. *Neuron.* 35:819–822.

Rubin, G.M., and A.C. Spradling. 1982. Genetic transformation of *Drosophila* with transposable element vectors. *Science.* 218:348–353.

Sapp, E., C. Schwarz, K. Chase, P.G. Bhide, A.B. Young, J. Penny, J.P. Vonsattel, N. Aronin, and M. Difiglia. 1997. Huntingtin localization in brains of normal and Huntington's disease patients. *Ann. Neurol.* 42:604–612.

Saudou, F., S. Finkbeiner, D. Devys, and M.E. Greenberg. 1998. Huntingtin acts in the nucleus to induce apoptosis but death does not correlate with the formation of intranuclear inclusions. *Cell.* 95:55–66.

Schweichel, J.U., and H.J. Merker. 1973. The morphology of various types of cell death in prenatal tissues. *Teratology.* 7:253–266.

Sperandio, S., I. de Belle, and D.E. Bredesen. 2000. An alternative, non-apoptotic form of programmed cell death. *Proc. Natl. Acad. Sci. USA.* 97:14376–14381.

Steffan, J.S., A. Kazantsev, O. Spasic-Boskovic, M. Greenwald, Y.Z. Zhu, H. Gohler, E.E. Wanker, G.P. Bates, D.E. Houseman, and L.M. Thompson. 2000. The Huntington's disease protein interacts with p53 and CREB-binding protein and represses transcription. *Proc. Natl. Acad. Sci. USA.* 97:6763–6768.

Strano, S., G. Fontemaggi, A. Costanzo, M.G. Rizzo, O. Monti, A. Baccarini, G. DelSal, M. Levrero, A. Sacchi, M. Oren, and G. Blandino. 2002. Physical interaction with human tumor-derived p53 mutants inhibits p63 activities. *J. Biol. Chem.* 277:18817–18826.

Sudol, M., H.I. Chen, C. Bougeret, A. Einbond, and P. Bork. 1995. Characterization of a novel protein-binding module – the WW domain. *FEBS Lett.* 369:67–71.

Sugars, K.L., and D.C. Rubinsztein. 2003. Transcriptional abnormalities in Huntington disease. *Trends Genet.* 19:233–238.

Tagawa, K., M. Hoshino, T. Okuda, H. Ueda, H. Hayashi, S. Engemann, H. Okado, M. Ichikawa, E.E. Wanker, and H. Okazawa. 2004. Distinct aggregation and cell death patterns among different types of primary neurons induced by mutant huntingtin protein. *J. Neurochem.* 89:974–987.

Taylor, J.P., J. Hardy, and K.H. Fischbeck. 2002. Toxic proteins in neurodegenerative disease. *Science.* 296:1991–1995.

Terrinoni, A., M. Ranalli, B. Cadot, A. Leta, G. Bagetta, K.H. Vousden, and G. Melino. 2004. p73-alpha is capable of inducing scotin and ER stress. *Oncogene.* 23:3721–3725.

Wyllie, A.H., and P. Goldstein. 2001. More than one way to go. *Proc. Natl. Acad. Sci. USA.* 98:11–13.

Yagi, R., L.-F. Chen, K. Shigesada, Y. Murakami, and Y. Ito. 1999. A WW domain-containing Yes-associated protein (YAP) is a novel transcription co-activator. *EMBO J.* 18:2551–2562.

Zoghbi, H.Y., and H.T. Orr. 2000. Glutamine repeats and neurodegeneration. *Annu. Rev. Neurosci.* 23:217–247.

ELSEVIER

Parkinsonism and Related Disorders 11 (2005) S17–S23

Parkinsonism & Related Disorders

www.elsevier.com/locate/parkreldis

The nature of the parkinsonism-dementia complex and amyotrophic lateral sclerosis of Guam and magnesium deficiency

Kiyomitsu Oyanagi*

Department of Neuropathology, Tokyo Metropolitan Institute for Neuroscience, 2-6 Musashidai, Fuchu, Tokyo 183-8526, Japan

Received 2 February 2005; revised 14 February 2005; accepted 14 February 2005

Abstract

The parkinsonism-dementia complex (PDC) and amyotrophic lateral sclerosis (ALS) were the fatal neurological diseases, showing very high incidence during 1950–1970 and dramatic decrease after 1970 on Guam. Through the research, the present author insisted that; (1) NFTs in Guam ALS patients are merely a background feature widely dispersed in the population, (2) Guam ALS and PDC are basically different diseases, and (3) Guam ALS occurs initially as classic ALS. As pathogeneses of the diseases, intake of low calcium (Ca) and magnesium (Mg) and high aluminum water and of some plant excitatory neurotoxin has been speculated. To elucidate the pathogenesis, the author performed an experiment exposing rats to low Ca and/or Mg intake for two generations, so as to follow the actual way of human living on the island, since several generations live continuously in the same environment. The study indicates that continuous low Mg intake for two generations induces exclusive loss of dopaminergic neurons in in rats, and may support the Mg hypothesis in the pathogenesis of PDC of Guam.

Keywords: Guam; Parkinsonism-dementia complex; Amyotrophic lateral sclerosis; Magnesium deficiency

1. Introduction

The Chamorro population on Guam in the western Pacific Ocean had represented about fifty times of the annual incidence rate of amyotrophic lateral sclerosis (ALS) as compared with the average in the world during 1950–1970 [1], and the rate of the parkinsonism-dementia complex (PDC) [2,3], which is a disease reported exclusively in Guam, Kii peninsula in Japan and west New Guinea, was also very high in the almost same period in Guam. Malamud et al. [4] and Hirano et al. [5] proposed that the ALS of Guam and Guam PDC are a single disease entity, and that Guam ALS is a disease different from classic ALS, because (i) the topographic distribution of NFTs and neuronal loss is similar to that of Guam PDC, (ii) patients with combined PDC and ALS (PDC–ALS) have been identified, and (iii) ALS as well as PDC patients are sometimes admixed within the same family. Regarding to the definition and pathogenesis of the diseases, the author intends to elucidate the nature of these fatal diseases, such as PDC and ALS, and performed an experimental study using rats exposing low magnesium (Mg) and/or calcium (Ca) for two generations.

2. Epidemiology

The maximum annual incidence rate of ALS of Guam from 1945 to 1955 was reported to be about 60–70 per 100,000 for men and 30–40 per 100,000 for women, and that of PDC in Guam from 1950 to 1970, to be about 60 for men and 20 for women [6,7]. The annual incidence rate of ALS was quite different among villages, from 0 to 250 per 100,000 population [1]. Although precise epidemiologic study is scant on Guam before the World War II, patients with ALS and/or PDC might exist on Guam from the far past, but it is evident that the annual incidence rate of these diseases on Guam has decreased remarkably after the World War II within short duration.

The mortality rate of PDC in Chamorro people on Saipan, a northern island of Guam, whose genotypic

* Tel.: +81 42 325 3881x4711; fax: +81 42 321 8678.
E-mail address: k123ysm@tmin.ac.jp.

1353-8020/$ - see front matter © 2005 Elsevier Ltd. All rights reserved.
doi:10.1016/j.parkreldis.2005.02.010

composition is similar to Guam Chamorro, was strikingly low suggesting an environmental risk factor [8]. Filipino migrants to Guam are susceptible to the disease further supporting an environmental over genetic etiology [9]. The increased risk to spouses of affected individuals in a longitudinal case-control study also strongly implicated environmental factors [10]. Since 1965, the incidence rate of Guam PDC has been decreasing, especially in men, but has remained at about 10–25 per 100,000 when last estimated for the period of 1980–1990 [6,7]. These findings suggest that environmental factors in combination with possible genetic risk factors may predispose to Guam PDC and account for the decreasing incidence in recent years. Similarly, the incidence rate for ALS has markedly decreased in recent years and is now similar to the rate in the rest of the world, namely about 3–5 per 100,000 [11].

3. Clinical symptoms

3.1. Parkinsonism-dementia complex

Patients with PDC are characterized by rigidity, tremor, bradykinesia and dementia in the fifth to sixth decade of life, and progression to a vegetative state with pelvicrural flexion contractures within 4–6 years [2,12]. About 40% of the patients with PDC, have clinical evidence of diabetes mellitus and hypertension before the onset of PDC [13].

3.2. Amyotrophic lateral sclerosis and ALS–PDC

Clinical symptoms of the patients with ALS of Guam have been reported to be essentially similar to those of the classic ALS. Average of onset of the disease was 47 years in male and 42 years in female, and spasticity had been reported to be the single initial feature in 13% of the patients [14], and 10% of the ALS patients lived at least 10 years [14]. Pyramidal tract sign was remarkable, but many patients lacked lower motor neuron signs of the lower extremities. Patients with long duration of the disease showed marked spasticity in the legs [15]. It has been reported that 5% of the patients with ALS subsequently developed the total clinical pictures of PDC (ALS–PDC), while 38% of the original PDC patients eventually developed typical ALS (PDC–ALS). Those ALS–PDC and PDC–ALS patients showed mixture of the symptoms of ALS and PDC [14].

4. Neuropathological findings

4.1. Parkinsonism-dementia complex

4.1.1. Macroscopic findings

The brain weight of PDC patients is reduced to be about 1070 g [16]. The cerebrum shows diffuse atrophy accentuated in the frontal and temporal lobes. The thickness of the cerebral cortex is generally reduced, especially in the hippocampus and parahippocampal gyrus. The hemispheric white matter is diffusely atrophic. The basal ganglia and thalamus are less severely deteriorated. The midbrain and pons show as severe atrophy as in the cerebrum (Fig. 1). There is marked depigmentation of substantia nigra and locus ceruleus. The volume of the cerebellum is preserved [16,17].

4.1.2. Neuronal loss and neurofibrillary tangles (NFTs)

The topographic distribution of neuronal loss and NFTs roughly coincide with that of brain atrophy [16,18–20]. Severe loss of neurons is seen in the CA1, and severe to moderate loss is observed in the temporal, insular and frontal cortices. Many NFTs are observed in the CA1, parahippocampal gyrus, temporal neocortex, and frontal cortex. The NFTs are predominantly distributed in the superficial layers of the cerebral cortex [21]. A great number of granulovacuolar degeneration and many Hirano bodies are seen in Ammon's horn. Except in a few cases, there are only small numbers of senile plaques [3,16,20,22]. Curly fibres/neuropil threads are rarely seen [16,22]. The cerebral white matter shows severe atrophy, but myelin pallor and threads are not remarkable in the cerebral white matter of most cases.

The number of large neurons in the neostriatum and the nucleus accumbens decreases to 40 and to10% of the control level, respectively. Large neurons correspondingly decrease in the basal nucleus of Meynert [23]. The globus pallidus shows a moderate neuronal loss and density of NFTs. Many alpha-synuclein positive neuronal inclusions and neurites are observed chiefly in the amygdaloid nucleus, and frequently coexist with tau-positive pretangles and NFTs in the same neurons [24]. The thalamus shows moderate neuronal loss and NFTs in the lateral nucleus and mild loss of neurons with some NFTs in the medial nucleus. Severe loss of neurons and many NFTs are present in the hypothalamus [3,16,18].

Severe loss of pigmented and nonpigmented neurons and presence of NFTs are observed in the substantia nigra [3,16,25], ventral tegmental area, locus ceruleus and superior central nucleus. Lewy bodies are rare. The pedunculopontine and pontine nuclei show many NFTs with mild neuronal loss [19].

Purkinje and granule cells are preserved in number. Although a small number of NFTs are observed in the dentate nucleus; no neuronal loss is evident and no grumose degeneration is seen [16]. No marked degeneration is observed in the cerebellar and spinal white matter. The spinal anterior horn cells appear shrunken, but are not reduced in number. A small number of NFTs composed of STs are observed in the intermediate zone and posterior horn, and occasionally in the anterior horn [3,16,19].

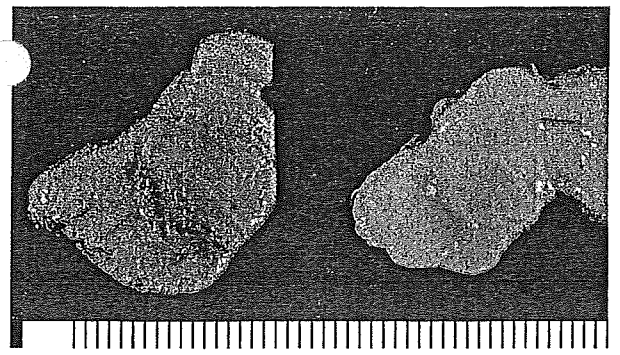

Fig. 1. Midbrain of the parkinsonism-dementia complex. Atrophy of midbrain and severe depigmentation of the substantia nigra was seen in a patient with PDC (right) comparing with an age-matched control Guamanian (left).

4.1.3. Ultrastructure and biochemistry of NFTs

NFTs are immunopositive for tau [16], and are mostly composed of paired helical filaments (PHFs) and partly of aight tubules (STs) in the Ammon's horn [19,26]. The remaining large neurons in the neostriatum frequently contain NFTs composed mainly of PHFs and partly of STs [23]. NFTs in the spinal cord were composed of STs [19]. A major tau triplet, 55, 64 and 69 kDa, and a minor variant at 74 kDa are the components of tau protein of NFTs in Guam PDC [27,28].

4.1.4. Glial inclusions

Tau-immunopositive and Gallyas-positive glial inclusions are observed in the patients with PDC. Granular hazy inclusions are observed in the astrocytes predominantly in the amygdaloid nucleus, motor cortex, and inferior olivary nucleus [29]. Coiled/crescent bodies are present in the oligodendroglia of the anterior nucleus of the thalamus, motor cortex, midbrain tegmentum, and the pyramids [29].

4.2. Amyotrophic lateral sclerosis and ALS–PDC

Essential neuropathological findings of the patients with ALS on Guam are those reported in the classic ALS. Neuronal degeneration is fundamentally restricted to the upper and lower motor neuron system. Lateral and anterior corticospinal tracts in many of the patients with ALS showed degeneration with preservation of the posterior funiculus. Bunina bodies and skein inclusions are frequently observed in the spinal anterior horn cells and facial and hypoglossal nuclei [16,19,20,30]. Ubiqutinated inclusion bodies (so-called motor neuron disease-inclusion) in the dentate gyrus and neuronal loss in the subiculum are not remarkable.

However, in addition to these findings, patients with ALS on Guam frequently showed NFTs and neuronal loss in the areas whose topographic distribution is similar to that of PDC [19].

5. Differential diagnosis and the nature of PDC and ALS on Guam

5.1. Parkinsonism-dementia complex

The large amount of NFTs with relatively small number of neuropil threads and glial tangles in Guam PDC is different from the widespread threads and glial tangles in the grey and white matter found in progressive supranuclear palsy (PSP), corticobasal degeneration (CBD) and frontotemporal dementia and parkinsonism linked to chromosome 17 (FTDP-17). The mild loss of neurons in the subthalamic nucleus, absence of grumose degeneration in the dentate nucleus and rare tuft-astrocytes in Guam PDC are different from PSP. Topographic distribution of loss of neurons in the substantia nigra is different from those in PSP and CBD [25] (Fig. 2). The absence of astrocytic plaques and ballooned neurons, and the small number of pretangles and foamy spheroid bodies in Guam PDC are different from CBD [20]. Astrocytic inclusions in PEP have been reported to be restricted to within the third ventricle wall and the periaqueductal area. Granular hazy astrocytic inclusions have been exclusively reported in Guam PDC [20,29].

5.2. Amyotrophic lateral sclerosis and ALS–PDC

As described above, it has been proposed that the ALS of Guam and Guam PDC are a single disease entity, and that Guam ALS is a disease different from classic ALS [4,5]. To elucidate the fundamental differences and similarities of the neuropathological features and etiopathogenesis of PDC and ALS of Guam, the author conducted a topographic and quantitative investigation of NFTs in 61 areas of the brains in 7 Guam ALS patients, 6 PDC patients, 3 ALS-PDC combined patients, and 20 non-ALS non-PDC Guamanians. NFTs were observed in 75% of non-ALS non-PDC Guamanian subjects, and in 86% of Guam ALS patients. The numbers of NFTs in the non-ALS non-PDC subjects and in ALS patients were the same, and less than that of PDC patients. The number of NFTs in ALS-PDC was the same as in PDC [19]. These findings indicate that;

(1) NFTs broadly occur in Guamanians living on Guam,
(2) NFTs in Guam ALS patients are merely a background feature widely dispersed in the population,
(3) Guam ALS and PDC are basically different diseases,
(4) Subtraction of the NFTs and related neuronal loss from the neuropathological findings of Guam ALS reveals findings of classic ALS,

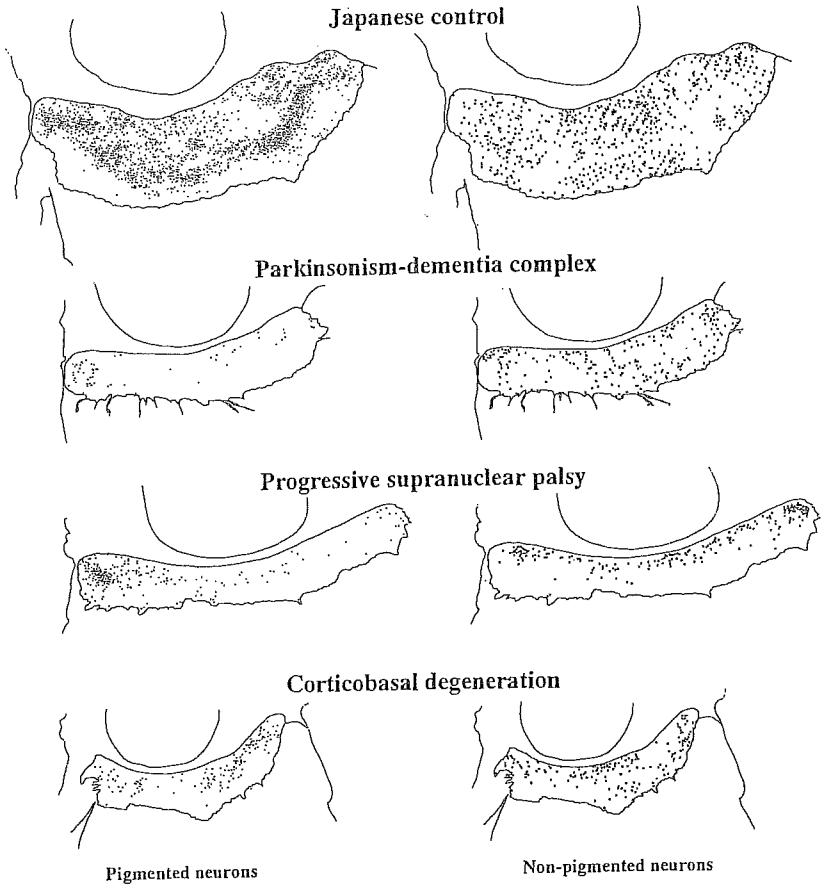

Fig. 2. Topographic distribution of loss of neurons in the substantia nigra. (Cited from Ref. [25]).

(5) ALS–PDC patients are considered to be combined cases of ALS and PDC. In other words, association of NFTs to the non-ALS non-PDC subjects and patients with ALS over the certain threshold level, brings them to PDC or ALS–PDC.
(6) Guam ALS occurs initially as classic ALS.

Summary of the discussion [19,20]:

(1) Guam ALS − NFT = Classic ALS
(2) Classic ALS + NFT = Guam ALS
(3) Classic ALS + many NFT = ALS–PDC
(4) Guam ALS = Initially classic ALS
(5) Guam ALS ≠ PDC

6. Pathogenesis

6.1. Genetics

No mutation of the tau gene has been found in PDC patients [31]. The percentage of subjects with the homozygous tau allele A0 is somewhat higher in Chamorro controls and PDC patients than Caucasian controls [32]. The representation of the G-to-C mutation in exon 9 of the CYP2D6 gene, linked to a slower metabolism of exogenous toxins, is higher in Chamorro control subjects and PDC patients than in Caucasian controls, and the apolipoprotein E2 allele frequencies in Chamorro controls and Guam PDC patients are considerably lower than those in Caucasian controls [33].

6.2. Environmental factors and experimental study

Infectious causes have been contradicted by the intense study by NIH, USA. Eventually intake of low Mg and Ca and high Al water [34] and of some plant neurotoxins (from cycad flour) [35], and a certain genetic predisposition [36] have been proposed. Recently another neurotoxin hypothesis from cycad rumphii via flying fox dish was proposed. The paper stressed high condensation of the toxin in bats [37].

Based on these possible pathogeneses proposed, experimental studies focusing on low Mg and Ca and high Al, and on plant neurotoxins have been explored. Repeated oral administration of alpha-amino-beta-methylaminopropionic acid (L-BMAA), the proposed toxic factor within flour of

cycad circinalis, to macaques produces chromatolysis of Betz cells, simple atrophy of spinal anterior horn cells and neuritic swelling in the substantia nigra [35], and a low-Ca, high-Al diet in monkeys induces neurofibrillary pathology characterized by accumulation of phosphorylated neurofilaments in the anterior horn cells [38]. A low-Ca and Mg, high-Al diet in mice for long duration of 11–31 months, induces loss of neurons and occurrence of tau-immunopositive neurons in the cerebral cortex [39]. Despite decades of research, no animal model completely recapitulates PDC or ALS. However, most of these experiments used adult or infantile animals in one generation.

7. Nigral degeneration in rats with magnesium (Mg) deficiency for two generations

Symptoms of the PDC and ALS occur at 50 or 60th in the life, and the patients with the diseases cannot to start to intake the water or the cycad flour at the ages. The present author performed an experiment using rats with long duration exposure of low Ca and/or Mg intake for two generations, in order to reproduce the actual way of life on the island, i.e. several generations live in the same circumstances.

Wistar albino rats were used. For elucidation of the critical period, which will induce lesions in the rats later, five groups with different exposure time were settled.

In this experiment, the foods were compounded with these trace metals in six different ratios. Distilled and deionized milli-Q water was given to drink. The food and water were given ad libitum. Number of experimental groups are 60, and examined number of rats was totally about 1000.

Historically the most significant changes were observed in the substantia nigra at 1 year. The substantia nigra of the rats, which was exposed to continuous Mg deficiency (one-fifth of the normal Mg level) till 1 year starting before mating, showed marked atrophy. The neurons decreased in number, and appeared small in size. Immunohistochemistry for tyrosine hydroxylase (TH) revealed that the size and number of TH-immunopositive neurons were small, and the number of TH-immunopositive dendrites or axons of the substantia nigra decreased severely in 1-year-old rats in this experimental group.

GFAP-immunopositive reactive gliosis was also observed in the substantia nigra in rats of the group. Lewy bodies, neurofibrillary tangels and senile plaques were not evident in each group, revealed by immunohistochemistry for alpha-synuclein, tau, ubiquitin and beta-peptide.

It has been reported that dietary Mg deficiency plays a major role in the pathogenesis of ischemic heart disease in humans, congestive heart failure, cardiac arrythmia, vascular complications of diabetes mellitus, pre-eclampsia and hypertension. Mg deficiency, as a possible pathogenesis of neurological diseases, had been speculated in the PDC and ALS in Chamorro population on Guam. Findings reported in the present study lead to the conclusion that Mg deficiency for two generations in rats induces the degeneration of substantia nigra by involving the mitochondria, rER, and free ribosomes in the neurons.

Degree of loss of neurons in the substantia nigra, and developmental retardation were more evident in the group of low Mg intake than the group of both low Mg and Ca intake. The finding shows that solely Mg deficient diet is more fundamental than evenly deficient diet of both Mg and Ca for the degeneration of the neurons and physical development.

In the present study, motor neurons, such as anterior horn cells were unremarkable though the substantia nigra showed evident loss of neurons. This might indicate that the pathogenesis of ALS of Guam is different from that of PDC of Guam, as reported in neuropathological studies of the patients by the present authors.

Though neurofibrillary tangles were not identified, this study may support the Mg hypothesis for pathogenesis of PDC of Guam, and may indicate the possibility of prevention/treatment of parkinsonism by Mg intake.

Acknowledgements

The present author is indebted to Dr Kwang-Ming Chen, Guam Memorial Hospital, Guam, USA, Emeritus Professor Fusahiro Ikuta, Niigata Neurosurgical Hospital and Brain Research Center, Niigata, Japan, and Professor Asao Hirano, Montefiore Medical Center, New York, USA, for their encouragement to proceed this study, Dr Takao Makifuchi, National Saigata Hospital, Niigata, Japan, Dr Takashi Ohtoh, National Kohriyama Hospital, Fukushima, Japan, Professor Hitoshi Takahashi, Niigata University, Niigata, Japan, Dr Masayuki Yasui, Yasui Clinic, Wakayama, Japan, and Ms Emiko Kawakami, Dr Kae Kikuchi-Horie, Mr Kazuhiko Ohara, and Dr Masahiko Takada, Tokyo Metropolitan Institute for Neuroscience, and Dr Kentaro Ogata, Ida Hospital, Kanagawa, Dr Manabu Wada, Yamagata University, Yamagata, Dr Tameko Kihira, Wakayama Medical College, Wakayama, Mr Tomio Ichikawa, Niigata University, Niigata, Japan, for their help. This work was supported in part by grants from the Japanese Ministry of Education, Science, Sports and Culture (No. 14580735), and the Japanese Ministry of Health, Labor and Welfare, Research on Psychiatric and Neurological Diseases (H16-kokoro-017).

References

[1] Kurland LT, Mulder DW. Epidemiologic investigation of amyotrophic lateral sclerosis. 1. Preliminary report on geographic distribution, with special reference to the Mariana islands, including clinical and pathological observations. Neurology 1954; 4:355–78.

[2] Hirano A, Kurland LT, Krooth RS, Lessell S. Parkinsonism-dementia complex, an endemic disease on the island of Guam. I. Clinical features. Brain 1961;84:642–61.

[3] Hirano A, Malamud N, Kurland LT. Parkinsonism-dementia complex, an endemic disease on the Island of Guam. II. Pathological features. Brain 1961;84:662–79.

[4] Malamud N, Hirano A, Kurland LT. Pathonanatomic changes in amyotrophic lateral sclerosis on Guam. Special reference to the occurrence of neurofibrillary changes. Arch Neurol 1961;5: 401–15.

[5] Hirano A, Malamud N, Elisan TS, Kurland LT. Amyotrophic lateral sclerosis and parkinsonism-dementia complex on Guam. Further pathologic studies. Arch Neurol 1966;15:35–51.

[6] Garruto RM, Yanagihara RT, Gajdusek DC. Disappearance of high-incidence amyotrophic lateral sclerosis and parkinsonism-dementia on Guam. Neurology 1985;35:193–8.

[7] Okumura H, Chen K-M, Kurland LT. Recent epidemiologic study of amyotrophic lateral sclerosis (ALS) and parkinsonism-dementia complex (PDC) in Guam island. Jpn J Clin Ecol 1995;4: 24–8.

[8] Yanagihara RT, Garruto RM, Gajdusek DC. Epidemiological surveillance of amyotrophic lateral sclerosis and parkinsonism-dementia complex in the common-wealth of the Northern Mariana Islands. Ann Neurol 1983;13:79–86.

[9] Chen K-M, Makifuchi T, Garruto RM, Gajdusek DC. Parkinsonism-dementia in a Filipino migrant: a clinicopathologic case report. Neurology 1982;32:1221–6.

[10] Plato CC, Garruto RM, Fox KM, Gajdusek DC. Amyotrophic lateral sclerosis and parkinsonism-dementia on Guam: a 25-year prospective case-control study. Am J Epidemiol 1986;124:643–56.

[11] Chen K-M. Personal communication.

[12] Chen K-M, Chase TN. Parkinsonism-dementia. In: Vinken PJ, Bruyn GW, Klawans HL, editors. Handbook of clinical neurology, vol. 49. Amsterdam: Elsevier; 1985. p. 167–83. Revised series 5, Chap 8.

[13] Chen K-M, Murakami N, Gibbs Jr CJ, Gajdusek DC. A study on the natural history of amyotrophic lateral sclerosis and parkinsonism-dementia complex of Guam. Clin Neurol 1980;13: 161–70.

[14] Elizan TS, Hirano A, Abrams BM, Need RL, van Nuis C, Kurland LT. Amyotrophic lateral sclerosis and parkinsonism-dementia complex of Guam. Arch Neurol 1966;14:256–368.

[15] Nagano Y, Tsubaki T, Chen K-M. Amyotrophic lateral sclerosis on Guam. Part 2. Clin Neurol 1977;17:582–5.

[16] Oyanagi K, Wada M. Neuropathology of parkinsonism-dementia complex and amyotrophic lateral sclerosis of Guam: an update. J Neurol 1999;246(Suppl 2):II/19–II/27.

[17] Oyanagi K, Makifuchi T, Ohtoh T, Ikuta F, Chen K-M, Chase TN, Gajdusek DC. Topographic investigation of brain atrophy in parkinsonism-dementia complex of Guam: a comparison with Alzheimer's disease and progressive supranuclear palsy. Neurodegeneration 1994;3:301–4.

[18] Hirano A, Zimmerman HM. Alzheimer's neurofibrillary changes. A topographic study. Arch Neurol 1962;17:227–42.

[19] Oyanagi K, Makifuchi T, Ohtoh T, Chen K-M, van der Schaaf T, Gajdusek DC, Chase TN, Ikuta F. Amyotrophic lateral sclerosis of Guam: the nature of the neuropathological findings. Acta Neuropathol 1994;88:405–12.

[20] Oyanagi K. Parkinsonism-dementia complex of Guam. In: Dickson D, editor. Neurodegeneration: the molecular pathology of dementia and movement disorders. Basel: ISN Neuropath Press; 2003. p. 137–42.

[21] Hof PR, Perl DP, Loerzel AJ, Morrison JH. Neurofibrillary tangle distribution in the cerebral cortex of parkinsonism-dementia cases from Guam: defference with Alzheimer's disease. Brain Res 1991; 564:306–13.

[22] Wakayama I, Kihira T, Yoshida S, Garruto RM. Rare neuropil threads in amyotrophic lateral sclerosis and parkinsonism-dementia on Guam and in the Kii Peninsula of Japan. Dementia 1993;4:75–80.

[23] Oyanagi K, Makifuchi T, Ohtoh T, Chen K-M, Gajdusek DC, Chase TN, Ikuta F. The neostriatum and nucleus accumbens in parkinsonism-dementia complex of Guam: a pathological comparison with Alzheimer's disease and progressive supranuclear palsy. Acta Neuropathol 1994;88:122–8.

[24] Yamazaki M, Arai Y, Baba M, Iwatsubo T, Mori O, Katayama Y, Oyanagi K. Alpha-synuclein inclusions in amygdala in the brains of patients with the parkinsonism-dementia complex of Guam. J Neuropathol Exp Neurol 2000;59:585–91.

[25] Oyanagi K, Tsuchiya K, Yamazaki M, Ikeda K. Substantia nigra in progressive supranuclear palsy, corticobasal degeneration, and parkinsonism-dementia complex of Guam: specific pathological features. J Neuropathol Exp Neurol 2001;60:393–402.

[26] Hirano A, Dembitzer HM, Kurland LT, Zimmerman HM. The fine structure of some intraganglionic alterations. Neurofibrillary tangles, granulovacuolar bodies, and 'rod-like' structures as seen in Guam amyotrophic lateral sclerosis and parkinsonism-dementia complex. J Neuropathol Exp Neurol 1968;27:167–82.

[27] Buée L, Delacourte A. Comparative biochemistry of tau in progressive supranuclear palsy, corticobasal degeneration, FTDP-17 and Pick's disease. Brain Pathol 1999;9:681–93.

[28] Mawal-Dewan M, Schmidt ML, Balin B, Perl DP, Lee VM-Y, Trojanowski JQ. Identification of phosphorylation sites in PHF-tau from patients with Guam amyotrophic lateral sclerosis/parkinsonism-dementia complex. J Neuropathol Exp Neurol 1996;55: 1051–9.

[29] Oyanagi K, Makifuchi T, Ohtoh T, Chen K-M, Gajdusek DC, Chase TN. Distinct pathological features of the Gallyas- and tau-positive glia in the parkinsonism- dementia complex and amyotrophic lateral sclerosis of Guam. J Neuropathol Exp Neurol 1997;56:308–16.

[30] Wada M, Uchihara T, Nakamura A, Oyanagi K. Bunina bodies in amyotrophic lateral sclerosis on Guam: a histochemical, immunohistochemical and ultrastructural investigation. Acta Neuropathol 1999; 98:150–6.

[31] Pérez-Tur J, Buée L, Morris HR, Waring SC, Onstead L, Vrièze FWD, Crook R, Buée-Scherrer V, Hof PR, Petersen RC, McGeer PL, Delacourte A, Hutton M, Siddique T, Ahlskog JE, Hardy J, Steele JC. Neurodegenerative diseases of Guam: analysis of tau. Neurology 1999;53:411–3.

[32] Conrad C, Andreadis A, Trojanowski JQ, Dickson DW, Kang D, Chen X, Wiederholt W, Hansen L, Masliah E, Thal LJ, Katzman R, Xia Y, Saitoh T. Genetic evidence for the involvement of tau in progressive supranuclear palsy. Ann Neurol 1997;41:277–81.

[33] Chen X, Xia Y, Gresham LS, Molgaard CA, Thomas RG, Galasko D, Wiederholt WC, Siatoh T. ApoE and CYP2D6 polymorphism with and without parkinsonism-dementia complex in the people of Chamorro, Guam. Neurology 1996;47:779–84.

[34] Yase Y. ALS in the Kii peninsula: one possible etiological hypothesis. In: Tsubaki T, Toyokura Y, editors. Amyotrophic lateral sclerosis. Tokyo: University of Tokyo Press; 1978. p. 307–18.

[35] Spencer PS, Nunn PB, Hugon J, Ludolph AC, Ross SM, Roy DN, Robertson RC. Guam amyotrophic lateral sclerosis—parkinsonism-dementia linked to a plant excitant neurotoxin. Science 1987;237: 517–22.

[36] Poorkaj P, Tsuang D, Wijsman E, Steinbart E, Garruto RM, Craig UK, Chapman NH, Anderson L, Bird TD, Plato CC, Perl DP, Wiederholt W, Galasko D, Schellenberg GD. TAU as a susceptibility gene for a amyotrophic lateral sclerosis-parkinsonism dementia complex of Guam. Arch Neurol 2001;58:1871–8.

[37] Banack SA, Cox PA. Biomagnification of cycad neurotoxins in flying foxes. Implications for ALS-PDC in Guam. Neurology 2003;61: 387–9.

[38] Garruto RM, Shankar SK, Yanagihara R, Salazar AM, Amyx HL, Gajdusek DC. Low-calcium, high-aluminum diet-induced motor neuron pathology in cynomolgus monkeys. Acta Neuropathol 1989; 78:210–9.

[39] Kihira T, Yoshida S, Yase Y, Ono S, Kondo T. Chronic low-Ca/Mg high-Al diet induces neuronal loss. Neuropathology 2002;22:171–9.

J Neuropathol Exp Neurol

Vol. 64, No. 10
October 2005
pp. 839–846

ORIGINAL ARTICLE

Tau-Positive Fine Granules in the Cerebral White Matter: A Novel Finding Among the Tauopathies Exclusive to Parkinsonism–Dementia Complex of Guam

Mineo Yamazaki, MD, PhD, Masato Hasegawa, PhD, Osamu Mori, MD, PhD, Shigeo Murayama, MD, PhD, Kuniaki Tsuchiya, MD, PhD, Kenji Ikeda, MD, PhD, Kwang-Ming Chen, MD, PhD, Yasuo Katayama, MD, PhD, and Kiyomitsu Oyanagi, MD, PhD

Abstract

We examined the autopsied brains of cases of 6 types of tauopathy: parkinsonism–dementia complex of Guam (PDC), corticobasal degeneration (CBD), progressive supranuclear palsy (PSP), Pick disease, Alzheimer disease (AD), and myotonic dystrophy together with Guamanian controls. Light microscopy sections of these brains were examined using anti-tau antibodies. Tau-positive fine granules (TFGs) were globe-shaped, and 3 to 6 μm in diameter, were observed predominantly in the frontal white matter in 30 of the 35 patients with PDC. However, no TFGs were found in association with PSP, myotonic dystrophy, Pick disease, AD, or CBD. Western blot analysis of frozen brain tissue taken from the PDC cases revealed that the frontal cortex was hyperphosphorylated and contained 6 tau isoforms (3R + 4R tau). However, in the present study, it was revealed that the novel TFGs in the white matter of patients with PDC was composed of 4R tau. Western blot analysis of sarkosyl-insoluble tau from the white matter of the PDC cases showed 2 major bands of 60 and 64 kDa and one minor band of 67 kDa. After dephosphorylation, these bands resolved into one major band of 4-repeat (4R) tau isoform and 3 minor bands of 3-repeat (3R) and 4R tau isoforms. Moreover, the TFGs observed in cases in which the number of neurofibrillary tangles (NFTs) was higher than the threshold level were not correlated with the presence of cortical NFTs. In conclusion, these novel TFGs were found almost exclusively in PDC brains and could therefore be considered as a characteristic neuropathologic marker of this particular tauopathy. The TFGs were hyperphosphorylated tau-positive structures that may be formed by a different mechanism from that used to produce cortical NFTs.

Key Words: Alzheimer disease, Corticobasal degeneration, Myotonic dystrophy, Parkinsonism–dementia complex of Guam, Pick disease, Tauopathies.

INTRODUCTION

Accumulations of hyperphosphorylated tau protein in neurons or glial cells are the hallmark lesions of a subset of neurodegenerative disorders that include corticobasal degeneration (CBD), progressive supranuclear palsy (PSP), Pick disease, Alzheimer disease (AD), argyrophilic grain disease (AGD), frontotemporal dementia with parkinsonism linked to chromosome 17 (FTDP-17) (1), and parkinsonism–dementia complex of Guam (PDC). These are referred to collectively as tauopathies. Biochemical and immunohistochemical analyses of tauopathy brains have shown that the morphologically distinct inclusions consist of either all 6 brain tau isoforms or the 3R tau or 4R tau isoforms only, depending on the disease (2).

Severe cerebral cortical atrophy is observed in the gray matter of PDC brains, as well as neuronal loss predominantly in the temporal and frontal lobes, and numerous neurofibrillary tangles (NFTs) with a distribution similar to that observed in AD brains (3, 4). The distribution of cortical NFTs predominantly in layers II and III in PDC brains is similar to that seen in PSP (5). The presence of granular hazy astrocytes has been reported by Oyanagi et al to be a specific neuropathologic marker of PDC (6). Thus far, no other specific marker for PDC has been found.

In contrast to the small number of tau-positive glial inclusions observed in the AD white matter, the PDC brains contained a substantial population of tau-positive glial inclusions such as argyrophilic threads, coiled bodies, and granular hazy astrocytes. During a precise examination of the PDC white matter, we observed tau-positive fine granules (TFGs). We investigated whether these structures were universal in all patients with PDC and examined whether they are specific to this particular tauopathy. Moreover,

From the Department of Neuropathology (MY, KO), Tokyo Metropolitan Institute for Neuroscience, Fuchu-shi, Tokyo; Department of Neurology (MY, YK) and 2nd Department of Pathology (OM), Nippon Medical School, Bunkyo-ku, Tokyo; Departments of Molecular Neurobiology (MH) and Psychogeriatrics (KI), Tokyo Institute of Psychiatry, Setagaya-ku, Tokyo; Department of Neuropathology (SM), Tokyo Metropolitan Institute of Gerontology, Itabashi-ku, Tokyo; Department of Laboratory Medicine and Pathology (KT), Tokyo Metropolitan Matsuazwa Hospital, Setagaya-ku, Tokyo, Japan; and Department of Neurology (K-MC), Guam Memorial Hospital, Guam.

Send correspondence and reprint requests to: Dr. Mineo Yamazaki, Department of Neuropathology, Tokyo Metropolitan Institute for Neuroscience, 2-6 Musashidai, Fuchu-shi, Tokyo 183-8526, Japan; E-mail: yamazaki@nms.ac.jp

This work was supported in part by a grant from the Japanese Ministry of Health, Labor and Welfare, Research on Psychiatric and Neurological Diseases (H16-kokoro-017 to KO) and a Grant-in-Aid for Research in Priority Areas from the Japanese Ministry of Education, Culture, Sports, Science and Technology (to MH).

a biochemical analysis of tau proteins in the white matter from patients with PDC was carried out to elucidate whether these TFGs are biochemically different from other tau-positive constituents.

MATERIALS AND METHODS

Cases

The present study was carried out using brains taken at autopsy from patients with PDC (n = 35), Guamanian PDC with amyotrophic lateral sclerosis (ALS; n = 4), Guamanian ALS (n = 7), Guamanian nonPDC, nonALS controls with neurologic disorders (n = 11), CBD (n = 10), PSP (n = 15), Pick disease (n = 4), AD (n = 10), AGD (n = 5), and myotonic dystrophy (n = 5; Table). Myotonic dystrophy was known to have NFTs in the neocortex and in subcortical nuclei (7). All of the Guamanian cases were examined and their condition diagnosed clinicopathologically by the authors (8–13). Some of the clinical and neuropathologic findings of the cases of CBD, PSP, Pick disease, AD, AGD, and myotonic dystrophy have already been reported elsewhere (14–26).

Histochemistry and Immunohistochemistry

The frontal white matter from autopsied brain tissue was cut into blocks, fixed in formalin, embedded in paraffin, and then sectioned at 4 μm. Some of these sections were stained with hematoxylin and eosin and by the Klüver-Barrera and Gallyas-Braak methods. The remaining sections were incubated with one of the following primary antibodies: anti-tau (AT8, monoclonal, 1:1000; Innogenetics, Temse, Belgium), anti-human tau (a gift from Professor Ihara, 1:1000; [27]), anti-ubiquitin (polyclonal, rabbit, 1:1000; Dako), and anti-glial fibrillary acidic protein (GFAP, polyclonal, rabbit, 1:1000; Dako). The immunolabeled sections were observed with the aid of a fluorescence microscope combined with a laser confocal system (TCS-SP; Leica, Heidelberg, Germany). For double immunostaining with anti-paired helical filaments (PHF) tau monoclonal (AT8, 1:1000; Innogenetics) and anti-GFAP/anti-ubiquitin/anti-phosphorylated neurofilaments (SMI31) antibodies, the specimens were blocked with nonimmune sera from horse or goat, depending on the secondary antibody used. Sections were first incubated with a mixture of the 2 primary antibodies and then with the fluorescence-labeled secondary antibodies (i.e. anti-mouse IgG coupled with fluorescein isothiocyanate [1:200; Cappel, Irvine, CA] and anti-rabbit IgG coupled with rhodamine [1:200; Cappel]).

TABLE. Summary of Cases Examined in This Study

Disease	Number	Gender of Cases	Age (years)
PDC of Guam (died 1979–1982)	35	23 male/2 female	64.4 ± 8.32
Guam PDC-ALS	4	2 male/2 female	63.0 ± 6.06
Guam ALS	7	3 male/4 female	52.1 ± 10.0
Guam control	11	4 male/7 female	68.8 ± 11.5
Corticobasal degeneration	10	4 male/6 female	65.7 ± 5.43
Progressive supranuclear palsy	15	8 male/7 female	74.4 ± 8.82
Pick disease	4	2 male/2 female	71.5 ± 3.70
Alzheimer disease	10	1 male/9 female	74.6 ± 15.1
Argyrophilic grain disease	5	3 male/2 female	82.4 ± 7.92
Myotonic dystrophy	5	3 male/2 female	54.4 ± 19.7

PDC, Parkinsonism–dementia complex; ALS, amyotrophic lateral sclerosis.

Quantitative Examination of Neurofibrillary Tangles and Tau-Positive Fine Granules

We performed quantitative analyses on the frontal subcortical white matter of brains from clinically diagnosed patients with PDC. The relationship between NFTs and TFGs was clarified by calculating the density of NFTs and TFGs in the frontal cortex of 12 patients with PDC. These 12 patients were sampled randomly from the 35 PDC cases examined in this study. With the aid of Gallyas-Braak staining, we computed the density of NFTs, including pretangles, in all layers of the 100-μm-wide frontal cortical ribbon. The number of TFGs in the center of the centrum semiovale in the frontal white matter was calculated by summing the number of TFGs in evenly distributed serial fields measuring 2.5 μm × 2.5 μm (giving a total area of 6.25 μm^2). The correlation between the density of NFTs and that of TFGs was estimated using Spearman's rank correlation coefficient. We used the Kruskal-Wallis test for comparing the density of NFTs with that of TFGs. Differences at $p < 0.05$ were considered significant.

Immunoelectron Microscopy

Paraffin-embedded, 6-μm-thick sections from the cerebral frontal white matter of PDC cases with tau-positive TFGs were immunostained with anti-tau antibody (AT8). The immunolabeling was visualized with diaminobenzidine (DAB), like for light microscope immunohistochemistry, and then processed for immunoelectron microscopy. After being post-fixed in 4% OsO_4 for 15 minutes, the sections were dehydrated in a graded ethanol series, embedded in epon 812, and then polymerized at 60°C for 24 hours. Ultrathin sections were cut and then stained with 3% lead acetate for 2 minutes and viewed with an electron microscope (H-9000; Hitachi, Japan) (28).

Biochemical Analysis

Frozen brain tissues from the frontal region, including both the gray matter and deep white matter of 4 PDC cases, one Guamanian ALS case with abundant TFGs in both the gray and white matter, one Guamanian control case, and 2 classic AD cases, were used for biochemical analysis. All of these brains were frozen at autopsy at –80°C. The gray and white matters were separated from each other macroscopically. Sarkosyl-insoluble tau was prepared according to a modification of the method of Goedert et al (29). Tissues were homogenized in a 10-fold (v/w) dilution of extraction buffer (10 mM Tris-HCl [pH 7.5], 1 mM EGTA, 0.8 M NaCl, 10% sucrose) and centrifuged at 23,000 × *g* for 20 minutes at 4°C. The pellets were rehomogenized in extraction buffer. Both of the 23,000 × *g* supernatants were combined, brought to 1% sarkosyl, and incubated for 1 hour at room temperature. After centrifugation at 113,000 × *g* for 20 minutes at 25°C, the

pellets were resuspended in 7 M guanidine-HCl and then dialyzed overnight against 30 mM Tris-HCl (pH 8.8). Dephosphorylation and immunoblotting were performed as described previously (30).

RESULTS

Microscope Study

The cerebral white matter of most patients with PDC exhibited no evident pallor with Kluver-Barrera stain. In addition to the TFGs, in the white matter of PDC (Fig. 1A, C), we found some tau-positive argyrophilic threads and coiled bodies. Some tiny tau-positive granular or thread-like structures with a diameter of 1 to 3 μm were also found in the PDC brains and in those of the other tauopathies studied here (Fig. 1B, D). These thread-like structures were found mainly in the frontal and temporal white matter and were not specific to PDC. They were also observed in the white matter of brains from patients with the other tauopathies examined in this study (AGD and CBD brain) and were clearly distinct from TFGs (Fig. 2A, B).

We observed TFGs in the frontal white matter of 30 of 35 patients with PDC (86%) and in 3 of 4 patients with PDC-ALS (75%). Moreover, only one of 7 Guamanian patients with ALS (14%) and 2 of 11 Guamanian controls (18%) whose cerebral cortices exhibited many NFTs also exhibited TFGs (Fig. 3). However, no TFGs were found in the brains of patients with myotonic dystrophy, Pick disease, or AD. In CBD brains, we found large numbers of argyrophilic threads and coiled bodies, but no TFGs (Fig. 2B). The TFGs were globe-shaped and approximately 3 to 6 μm in diameter, and were distinct from argyrophilic threads. TFGs were positive to both AT8 and anti-human tau antibodies (Fig. 1A, B), but some parts of them were not stained by the Gallyas-Braak method. Some TFGs consisted of globular dense tau-positive structures surrounded by weakly tau-positive fluffy materials (Fig. 1C). They were observed frequently in the frontal white matter, the frontal lobe, and the temporal subcortical white matter. In the PDC cases in which TFGs were abundant in the frontal white matter, some were also found in the frontal cortex. However, TFGs were only rarely observed in the spinal cord, cerebellum, or brainstem.

Confocal scanning microscope observations of immunofluorescence double-labeled sections showed that GFAP and phosphorylated neurofilament were not localized on TFGs (Fig. 4A, B). Although most of the TFGs exhibited no colocalization of ubiquitin and tau, it was observed on some (Fig. 4C). The pattern of this colocalization, when it was observed, varied from only a small part (i.e. the center) of the TFG to staining in almost all of it.

Quantitative Analysis of Tau-Positive Fine Granules and Neurofibrillary Tangles

We found no significant relationship between the number of NFTs and the number of TFGs. However, the 12 patients with PDC could be divided into 2 groups: those with more than 200 NFTs/100 μm-length of the frontal cortical ribbon and those with less (Fig. 5). The graph shown in Figure 4 shows that TFGs were only observed in those PDC cases with more than approximately 200 NFTs/100 μm-length of the frontal cortical ribbon. There was no significant

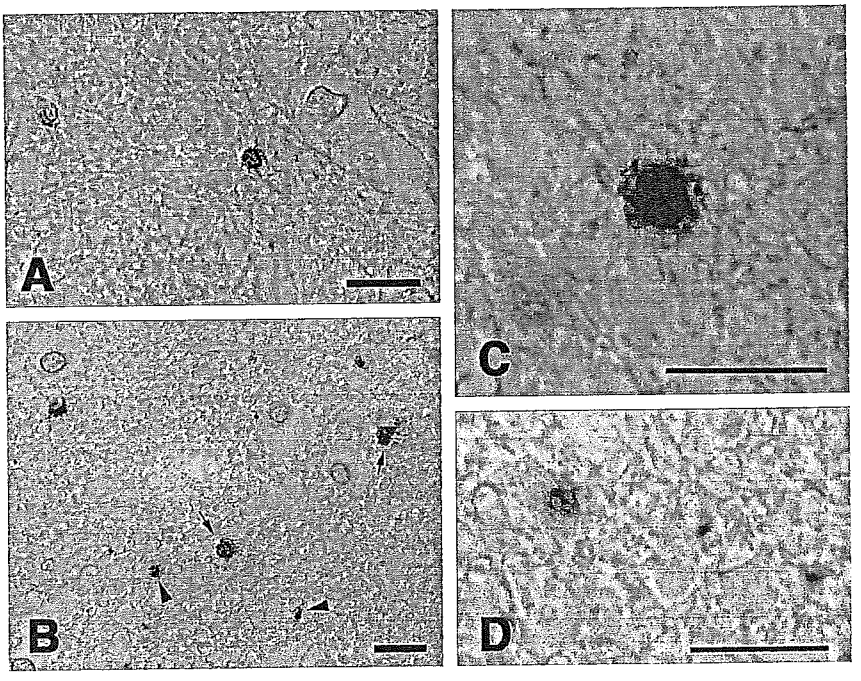

FIGURE 1. Immunohistochemical findings in the frontal white matter of parkinsonism–dementia complex of Guam (PDC) brains. Anti-tau antibodies (human tau [A] and AT8 [B]) were used to examine sections of the frontal white matter. (B) Tau-positive fine granules (TFGs) (arrows) are globe-shaped and approximately 3 to 6 μm in diameter, and are distinct from argyrophilic threads. They were observed frequently in the frontal white matter. Tiny tau-positive granular structures (arrowheads) of 1 to 3 μm in diameter were found in the PDC brains and those of other tauopathies. These structures are thus not specific to PDC and could be clearly distinguished from TFGs. High-power views of TFGs (C) and tiny tau-positive granular structures (D), both stained immunohistochemically for tau using AT8. (C) Some TFGs consisted of globular dense tau-positive structures surrounded by weakly tau-positive fluffy materials. Scale bars: 10 μm.

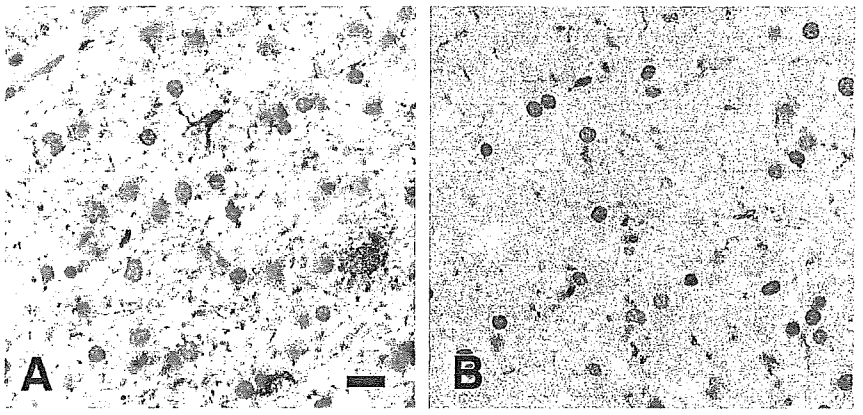

FIGURE 2. Immunohistochemical findings in the frontal white matter of brains with argyrophilic grain disease (AGD) (**A**) and corticobasal degeneration (CBD) (**B**) using anti-tau (AT8) antibody. Abundant tiny tau-positive granular structures were found, but no tau-positive fine granules were observed found in the frontal white matter of brains with AGD (**A**) and CBD (**B**). Scale bars: 10 μm.

correlation between the degree of white matter degeneration and the density of TFGs.

Immunoelectron Microscope Observations

Most of the AT8-positive TFGs had some contact with the myelin outer loop, but no TFGs were observed within the myelin sheath or the axons (Fig. 6A). High-power views of these sections revealed that TFGs contained round structures that were 20 to 30 nm in diameter (including the DAB substrate) (Fig. 6B). These structures were also observed near the nucleus of glial cells that were thought to be oligodendroglia (Fig. 6C, D).

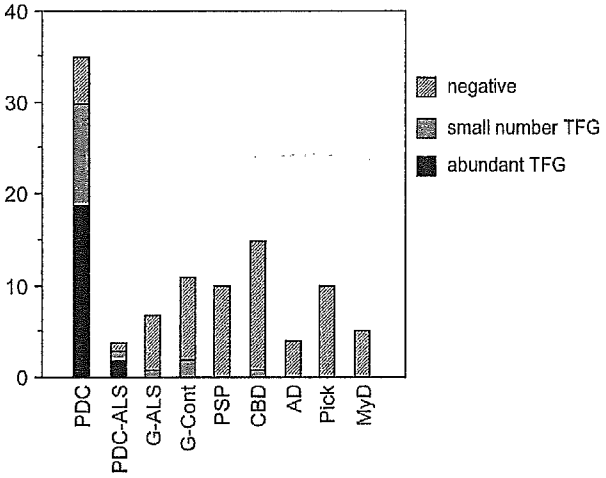

FIGURE 3. Tau-positive fine granules (TFGs) in the frontal white matter of brains with various tauopathies. Histogram showing the number of the cases having abundant TFGs (black), cases with only a small number of TFGs (narrow slash mark), and TFG-negative cases (broad slash mark) in each disease group. The density 50 TFGs/100 μm^2 marked the border between the "abundant TFGs" group and the "small number of TFGs" group. PDC, Parkinsonism–dementia complex; G-ALS, Guam amyotrophic lateral sclerosis; G-Cont, Guam control; CBD, corticobasal degeneration; PSP, progressive supranuclear palsy; AD, Alzheimer disease; Pick, Pick disease; MyD, myotonic dystrophy.

Biochemical Analysis

The sarkosyl-insoluble fraction prepared from the white matter of the frontal lobes of PDC cases that exhibited TFGs were analyzed by Western blotting with a the phosphorylation-independent anti-tau antibody HT-7. Two major bands were detected, one with an apparent molecular mass of 60 kDa and another of 64 kDa, and one minor band with an apparent molecular mass of 68 kDa. After dephosphorylation, these bands appeared as one major band corresponding to a 4-repeat tau isoform with zero amino acid inserts (4R0N) and 3 minor bands corresponding to a 4-repeat tau isoform with 29 amino acid inserts (4R29N), a 3-repeat tau isoform with zero amino acid inserts (3R0N), and a 3-repeat tau isoform with 29 amino acid inserts (3R29N; Fig. 7).

The insoluble tau extracted from the gray matter of cortices from the PDC cases resolved into 3 bands of apparent molecular mass 60, 64, and 68 kDa. Six bands were detected after dephosphorylation, corresponding to 6 tau isoforms that resembled those that were resolved in AD brains. Similar results were obtained from the analysis of another PDC case (PDC-4) and one Guamanian ALS case with abundant TFGs (data not shown). No insoluble tau was extracted from the frontal brain of a Guamanian control. Accumulations of both 3R and 4R tau isoforms were detected in the white matter of the PDC cases. However, when compared with tau in the gray matter, the levels of 4R tau isoforms were high and the levels of 3R tau isoforms were very low, which was different from those in the gray matter in which similar levels of 3R and 4R tau isoforms or slightly higher levels of 3R tau isoforms were detected. Furthermore, the 4R tau band pattern after dephosphorylation was most obvious in cases in which TFGs were abundant in the white matter. These results suggest that the TFGs in the white matter in the patients with PDC were composed predominantly of 4R tau isoforms.

Sarkosyl-insoluble tau from the white matter of AD brains consisted of a triplet of apparent molecular mass 60, 64, and 68 kDa, which resolved into 6 bands after dephosphorylation (data not shown), indicating that in AD, the tau isoforms deposited in the white matter (mostly in axons) were the same as those deposited in the gray matter, although there was far less of the pathologic tau in the white matter than in the gray matter.

DISCUSSION

TFGs are novel and unique tau-positive inclusions that we observed in the frontal white matter of 86% of the patients with PDC examined here. No TFGs were found in the brains of patients with myotonic dystrophy, Pick disease, or AD.

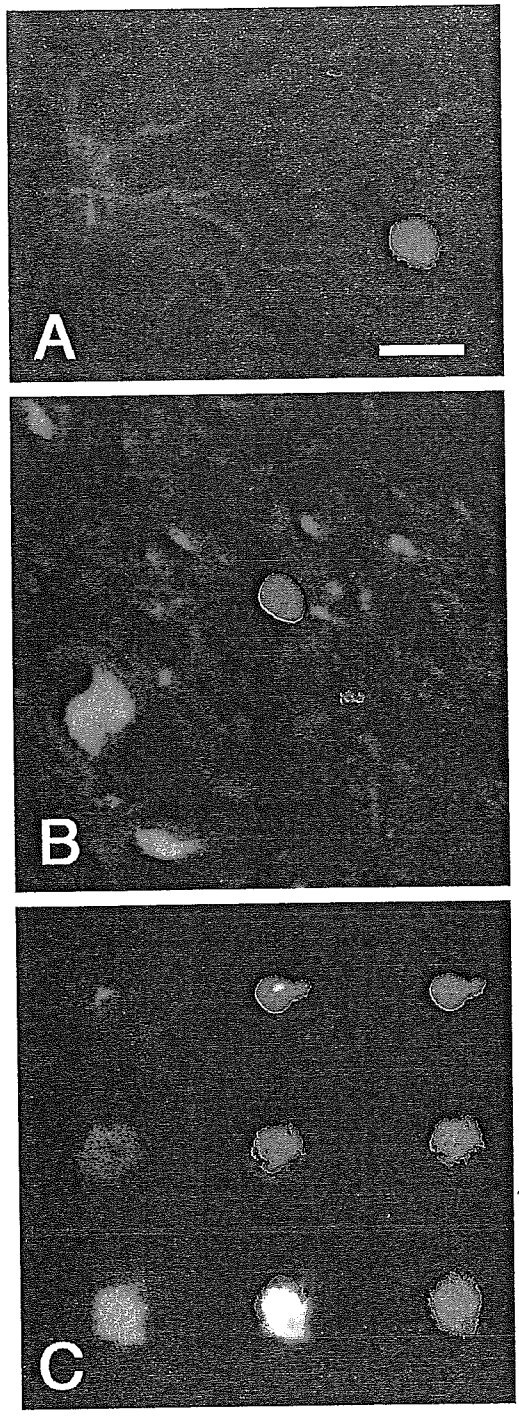

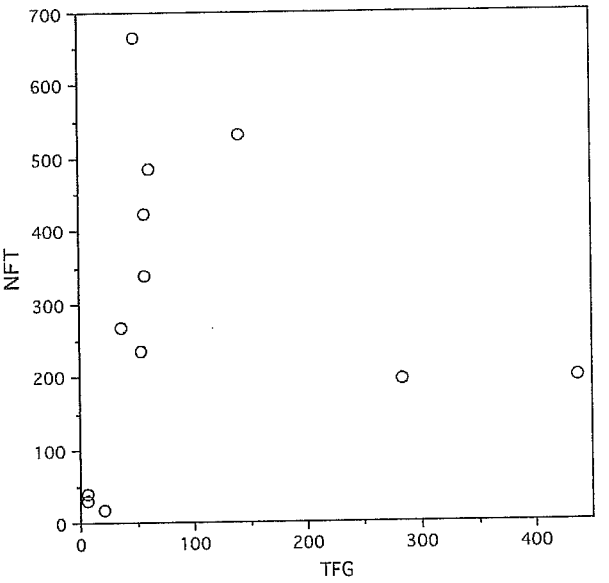

FIGURE 5. Relationship between the densities of neurofibrillary tangles (NFTs) and tau-positive fine granules (TFGs) in Guam parkinsonism–dementia complex (PDC). The number of TFGs was counted in a 100-μm^2 area of frontal white matter and the number of NFTs was counted in a 100-μm length of the frontal cortex. No significant relationship was found between the numbers of NFTs and TFGs in the frontal brains of patients with Guam PDC. However, it is safe to say that TFGs only seem to develop when the number of NFTs reaches a certain threshold level.

Furthermore, only a few of the Guamanian controls and Guamanian patients with ALS with many NFTs also exhibited TFGs. Globe-shaped and tau-positive inclusions like TFGs have never been described previously, although other tau-positive inclusions have been reported. Immunoelectron microscope observations revealed that putative TFGs are tau-positive structures that take the shape of granules with a diameter of 20 to 30 nm (including the DAB coating). The PDC white matter stained with Klüver-Barrera and Bodian did not mark a significant change in the stainability even in cases with many TFGs, despite atrophy of the white matter TFGs might relate to this peculiar degeneration of the PDC white matter. We became interested in whether the presence of TFGs had a connection to the atrophy of white matter in the PDC brain.

Immunofluorescence double labeling of TFGs, observed with the aid of confocal scanning microscopy, revealed no

FIGURE 4. Confocal scanning microscope observations made with the aid of immunofluorescence double labeling. GFAP ([A], green) and phosphorylated neurofilament ([B], green; SMI 31) were not localized on tau-positive fine granules (TFGs) (red; AT8). (C) Ubiquitin (green; left) was localized with tau (AT8, red; right) on TFGs in various distribution patterns (merged images) from only a small part (center) of the TFG to staining throughout most of the TFG (lower stand). Scale bars: 5 μm.